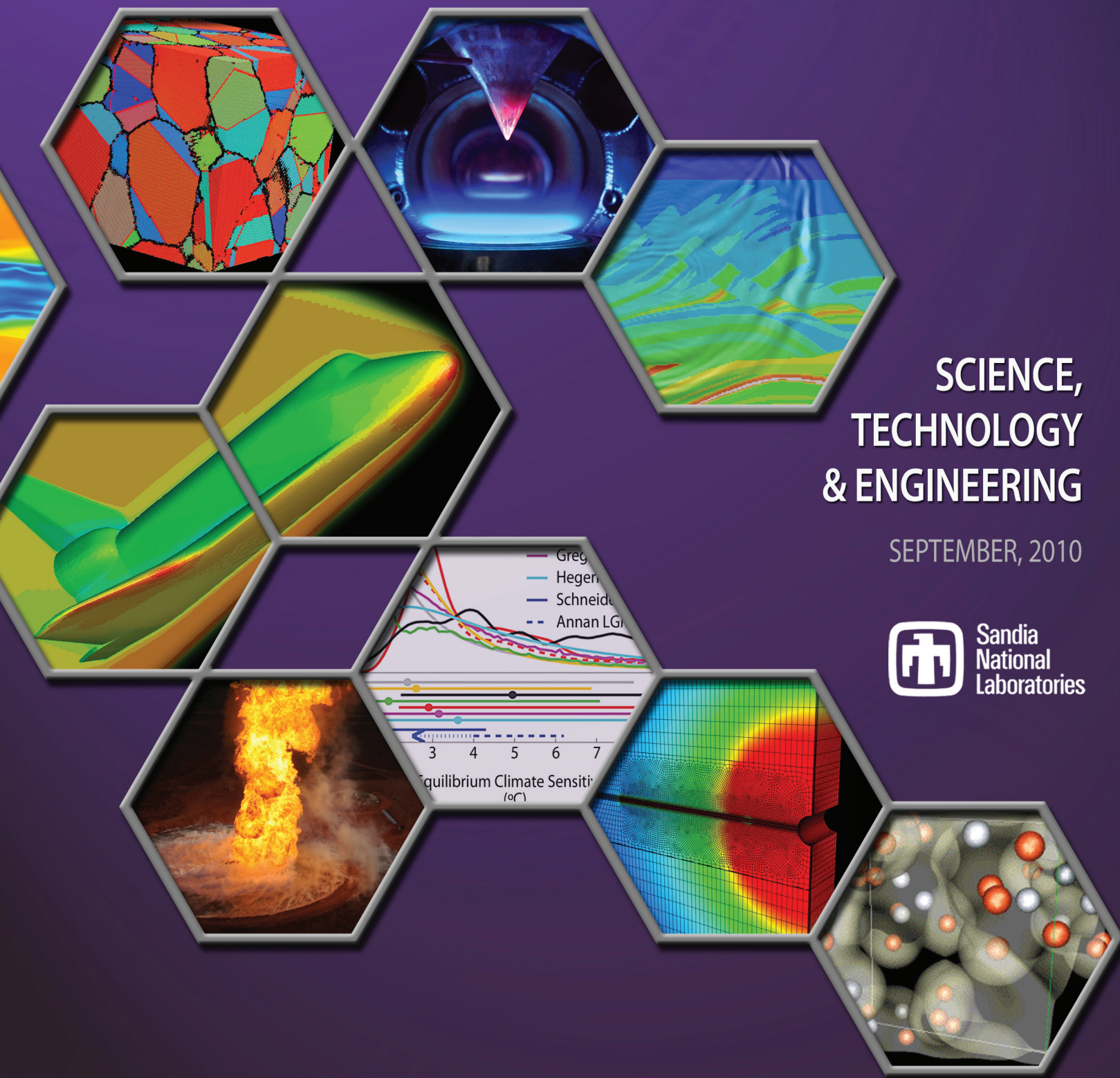


*Discovery at the Interface of
Science and Engineering:*

Science Matters!



SCIENCE,
TECHNOLOGY
& ENGINEERING

SEPTEMBER, 2010



Sandia
National
Laboratories

NOTICE: This report was prepared as an account of work sponsored by an agency of the United States Government. Neither the United States Government, nor any agency thereof, nor any of their employees, nor any of their contractors, subcontractors, or their employees, make any warranty, express or implied, or assume any legal liability or responsibility for the accuracy, completeness, or usefulness of any information, apparatus, product, or process disclosed, or represent that its use would not infringe privately owned rights. Reference herein to any specific commercial product, process, or service by trade name, trademark, manufacturer, or otherwise, does not necessarily constitute or imply its endorsement, recommendation, or favoring by the United States Government, any agency thereof, or any of their contractors or subcontractors. The views and opinions expressed herein do not necessarily state or reflect those of the United States Government, any agency thereof, or any of their contractors.

Printed in the United States of America. This report has been reproduced directly from the best available copy.

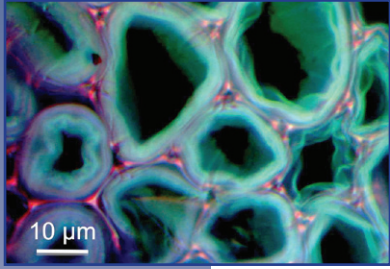


SAND2010-5893P 09/2010
Issued by Sandia National Laboratories, Albuquerque, New Mexico, USA for the
US National Nuclear Security Administration (NNSA) Office of Research &
Development for National Security Science & Technology, NA-121.

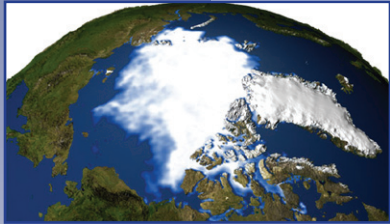
Sandia National Laboratories is a multi-program laboratory managed and operated by Sandia Corporation, a wholly owned subsidiary of Lockheed Martin Corporation, for the U.S. Department of Energy's National Nuclear Security Administration under contract DE-AC04-94AL85000.



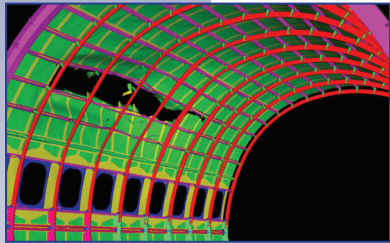
SANDIA NATIONAL LABORATORIES Science, Technology and Engineering



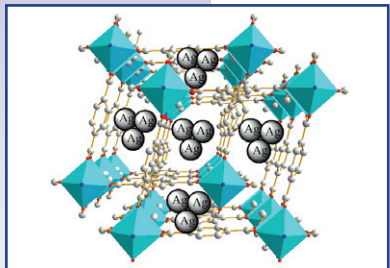
Bioscience



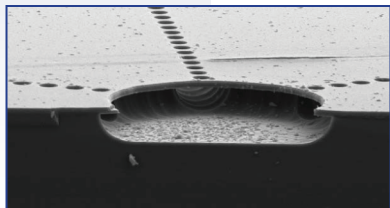
Computers and Information Sciences



Engineering Sciences



Materials Science and Technology



Microelectronics and Microsystems



Pulsed Power

Vision

Sandia National Laboratories is the provider of innovative, science-based, systems-engineering solutions to our Nation's most challenging national security problems.

Mission

Committed to "science with the mission in mind," Sandia creates innovative, science-based, systems-engineering solutions that

- sustain, modernize, and protect our nuclear arsenal,
- prevent the spread of weapons of mass destruction,
- provide new capabilities for national defense,
- defend against terrorism,
- protect our national infrastructures, and
- ensure stable sources of energy and other critical resources.

Guiding principles for ST&E

- Ensure that the fundamental science and engineering core is vibrant and pushing the forefront of knowledge
- Enable the programs by effective application of that science base
 - ♦ responding to current needs
 - ♦ anticipating the future

About Science Matters!

The purpose of *Science Matters!* is to publicize and celebrate recent Sandia accomplishments in science, technology, and engineering. We feature the science that underpins and enables technology for Sandia's missions. We nurture expertise, facilities and equipment to create world-class science that pushes the frontiers of knowledge and anticipates future mission needs. New *Science Matters!* are being issued semiannually.

Vice President & Chief Technology Officer
J. Stephen Rottler, Ph.D.
505-844-3882
jsrottl@sandia.gov

Deputy, Science & Technology
James Woodard, Ph.D.
505-845-9520
jwoodar@sandia.gov

Science Matters! Point of Contact
Alan Burns, Ph.D.
505-844-9642
aburns@sandia.gov





◀ FIGURE CAPTIONS

(Preceding page, from top to bottom)

Confocal fluorescence microscope image of switchgrass cell wall

Composite image of sea ice in the Arctic region acquired in 2003 by the Defense Meteorological Satellite Program Special Sensor Microwave Imager. Source: earthobservatory.nasa.gov

Simulation results showing tearing in an aircraft fuselage subjected to blast loading. Failure is represented using the “element death” technique.

Silver nanoparticles created in a metal organic framework (MOF).

Wet hydrogen fluoride etched buried guidance cues for neural networks on silicon chip. Scale bar = 10 μm .

Lightning caused the 2006 Sago mine disaster in West Virginia.

Contents

Computer and Information Sciences

Climate Uncertainty and Implications for U.S. State-Level Risk Assessment Through 2050 **4**
George Backus

Large-Scale Seismic Inversion **6**
Curtis C. Ober and
S. Scott Collis

To Protect Quantum Information, Understand What Threatens it **8**
Wayne M. Witzel and
Richard P. Muller

Combustion Science

Fundamentals of Biofuel Combustion Chemistry **10**
Nils Hansen

Engineering Sciences

The Phoenix Series of Liquefied Natural Gas Pool Fires **12**
Thomas K. Blanchat and
Michael M. Hightower

Quantum-Kinetic Approach for Modeling Non-Equilibrium Gas-Phase Chemical Reaction Rates **14**
Michael A. Gallis, Ryan P. Bond,
and John R. Torczynski

Vibration-Induced Gas-Liquid Effects in Accelerometers **16**
Timothy J. O'Hern
and John R. Torczynski

Coupled Multi-Physics Modeling to Support Energy R&D **18**
Mike Stone

Materials Science and Technology

How Grain Growth Stops: A New Solution to an Old Mystery **20**
Elizabeth A. Holm and
Stephen M. Foiles

Removable Encapsulants **22**
James R. McElhanon,
Edward M. Russick, and
James H. Aubert

The Role of Carbon Surface Diffusion on the Growth of Epitaxial Graphene on SiC **24**
Taisuke Ohta and
Norman C. Bartelt

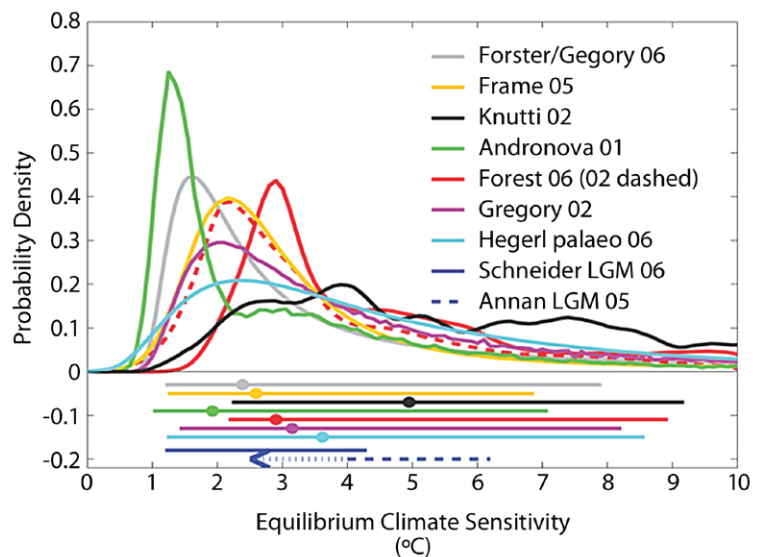
Hydrogen Storage Research in the Metal Hydride Center of Excellence **26**
Vitale Stavila and
Lennie Klebanoff

Computer and Information Sciences

Climate Change

Climate Uncertainty and Implications for U.S. State-Level Risk Assessment Through 2050

Figure 1: Uncertainty in climate change due to a doubling of atmospheric CO_2 . (Ref. 2). Shown here is the comparison between different estimates of the probability density (or relative likelihood) for climate sensitivity (i.e., temperature increase $^{\circ}\text{C}$). All the probability curves have been scaled to integrate to unity between 0°C and 10°C sensitivity. The bars show the respective 5 to 95% ranges and the dots the median estimate.



*Applying risk assessment
and uncertainty
quantification methods
to climate change
determines the avoidance
value of mitigation and
adaptation options.*

For more information:

Technical Contact:

George Backus
505-284-5787
gabacku@sandia.gov

Science Matters Contact:

Alan Burns
505-844-9642
aburns@sandia.gov

Although the existence of climate change is understood with a high degree of certainty, its extent and future dynamics remain highly uncertain. For example, the probability distributions of future global warming models (Figure 1), included in the 2007 Assessment Report from the United Nations' Intergovernmental Panel on Climate Changes (IPCC), are skewed heavily toward much larger temperature changes than the "best estimate" values commonly discussed for a doubling of CO_2 concentration in the atmosphere. The skewed probability distributions illustrate the uncertainty in future climatic conditions, which may be irreducible despite advances in climate science and the computational modeling of climate dynamics. Moreover, the large uncertainties create substantial risks if nothing is done to mitigate and/or prepare for climate change. Risk is the combination of potential consequences and the probability of those consequences occurring. Understanding the risks of

climate change is useful for policymakers to prioritize any actions that could avoid the realization of those risks. As shown here, the potentially realized higher temperature and adverse precipitation conditions implied by the climate change probability distribution pose disparate consequences for the states across the country.

The extensive systems integration capabilities at Sandia have been used by researchers to generate the first truly integrated assessment of climate risk among the contiguous 48 states. Multiple departments combined their expertise in uncertainty quantification, risk assessment, climate science, hydrology, infrastructure impacts, and macroeconomic analysis to develop a state-level risk assessment of climate change impacts through the year 2050. The most uncertain impact of the predicted climate change characteristic, *precipitation*, was used to assess economic impacts associated with water availability. Changes in water availability can have clear,

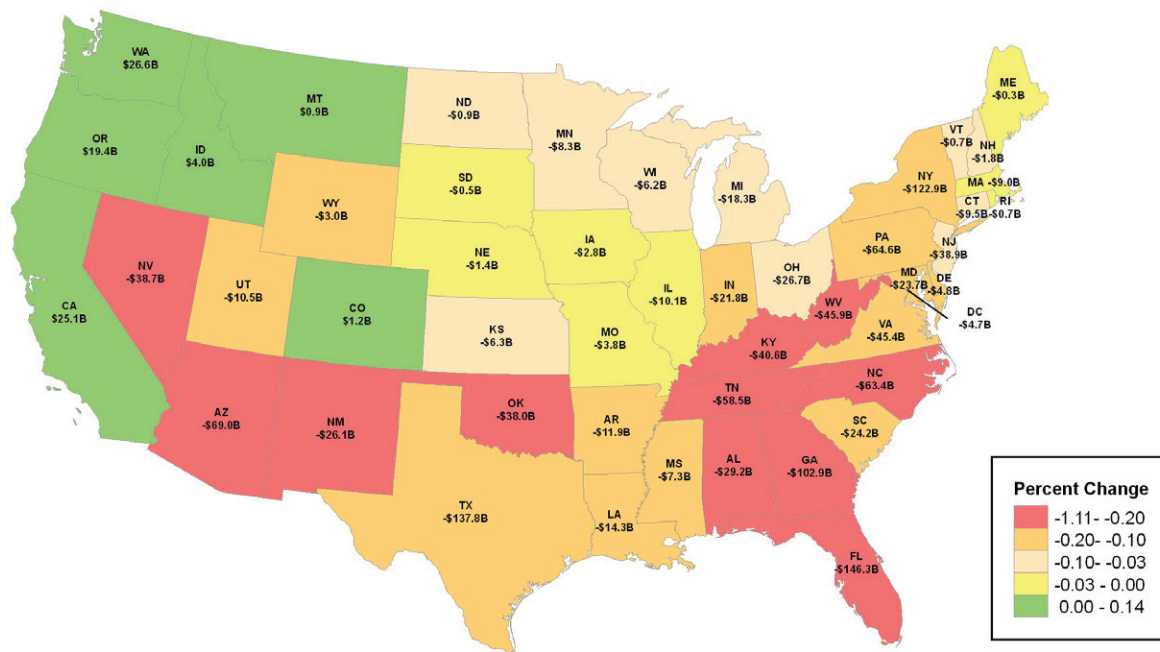


Figure 2: State-level economic impacts of climate change from 2010 through 2050, due to a doubling of CO₂ and the consequent changes in water availability. The colors represent various amounts of change in the economic activity (gross state products) of each state.

direct socioeconomic consequences; the summary risk is the integral of the consequence of reduced precipitation over the entire probability distribution of those precipitation conditions. Researchers then determined the implied hydrologic conditions using the Sandia Energy-Water model, followed by a determination of the economic impacts across interacting state-level economics, over time, for 70 industries using the macroeconomic analysis capabilities of Sandia's National Infrastructure Simulation and Analysis Center. Finally they combined the time-dependent, probabilistic, consequences to determine the risk for each for the 48 contiguous states.

At the national level, the risk between 2010 and 2050 is estimated to be \$1.2 trillion, with an employment loss of nearly seven million labor years. All states except the Pacific Northwest, California and Colorado show net negative impacts over the time period. The benefits to the Northwest may be overestimated due to the lack of intra-annual resolution on precipitation affecting snow cover within the analysis. Conversely, while California and Colorado do suffer the negative impacts from the loss of precipitation often noted in previous studies, worse conditions in surrounding states cause population in-migration that lead to a net benefit in California and Colorado economic conditions. In addition to the risk assessment and level of detail, this dynamic interaction among the states is a critical element that is missing from previously published studies of climate change impacts.

Figure 2 summarizes the state-level impacts of climate change on Gross State Product (GSP) from 2010 through 2050 in billions of 2008 dollars. Because Sandia is using the vantage point of the population experiencing the loss, the risk in cost terms is the actual value calculated rather than a discounted value. Any effort to mitigate the risk by actions today would consider the non-zero discount rates that reflect the time preference society uses to compare conditions today to future conditions.

References

1. Backus, G., T. Lowry, D. Warren, M. Ehlen, G. Klise, V. Loose, L. Malczynski, R. Rienhart, K. Stamber, V. Tidwell, V. Vargas, and A. Zagonel (2009), *Climate Uncertainty and Implications for U.S. State-Level Risk Assessment Through 2050*, SAND Report 2009-7001, Sandia National Laboratories, Albuquerque, NM
2. Solomon, S., D. Qin, M. Manning, Z. Chen, M. Marquis, K.B. Averyt, M. Tignor and H.L. Miller (eds.) 2007, *Contribution of Working Group I to the Fourth Assessment Report of the Intergovernmental Panel on Climate Change*, Cambridge University Press, Cambridge, United Kingdom and New York, NY, USA.

Computer and Information Sciences Simulation Technologies

Large-Scale Seismic Inversion

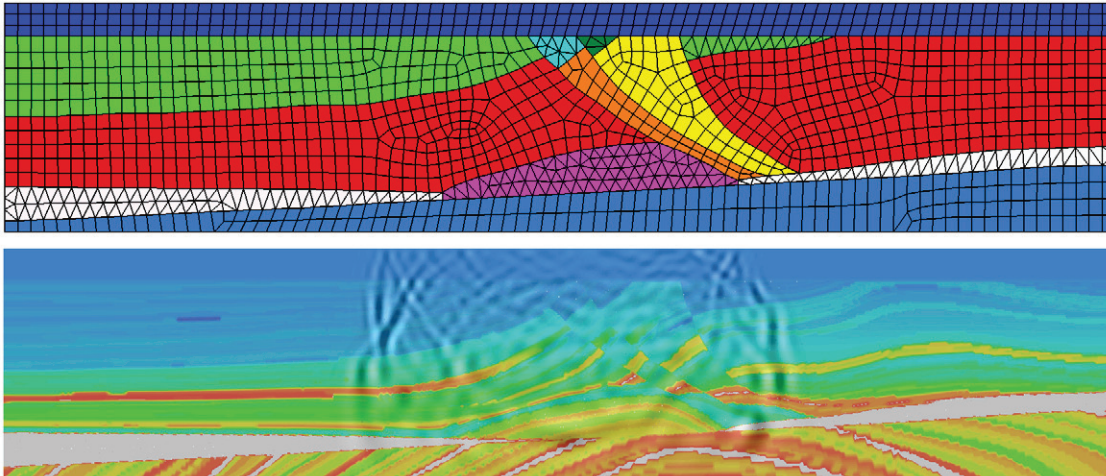


Figure 1: A hybrid triangular and quadrilateral unstructured mesh generated by Sandia's CUBIT for the Marmousi2 model (a standard seismic model with many layers, Reference 3) that conforms to geological interfaces (top), and simulated pressure waves propagating through the model (bottom).

Sandia is exploring new algorithmic approaches to modeling the complex geology of the earth's interior.

For more information:

Technical Contacts:

Curtis C. Ober
505-844-1846
ccober@sandia.gov

S. Scott Collis
505-284-1123
sscoll@sandia.gov

Science Matters Contact:

Alan Burns
505-844-9642
aburns@sandia.gov

Much of what is learned about the geology of the earth's interior is through seismic surveys that record reflected sound waves traveling through the various layers and structures. In "seismic inversion," one estimates the geologic structure and properties, density and wave speeds, and then simulates the seismic waves and surveys to produce synthetic recordings. These recordings are then compared to the actual field recordings to improve the initial estimates. This process is repeated until a sufficiently accurate earth model is obtained (Reference 2).

Advances in seismic inversion could have broad-reaching national impact for earthquake prediction, oil and gas exploration and production, carbon sequestration, nuclear-waste repositories, and nuclear non-proliferation monitoring. However, the process is a computational grand challenge. Discontinuous material interfaces, attenuation, and large-scale optimization are some of the major problems in the field today. Discontinuous material interfaces occur routinely in seismic surveys, such as the ocean bottom, salt structures, and faults (Figure 1 top). Sandia is leveraging advanced forward simulation methods, such as discontinuous

Galerkin (DG) methods on unstructured meshes, along with adjoint-based inversion algorithms, to solve seismic inversion problems on distributed-memory parallel computers.

DG methods are a numerical approach to solve partial differential equations (PDEs). They use techniques from finite element and finite volume methods, and easily extend to higher-order approximations for the PDEs. The solution is continuous within the element, but across element boundaries it is discontinuous. To handle these discontinuities, solutions to the Riemann problem are used. DG methods are well-suited to hyperbolic PDEs which model physics with seismic wave-propagation. DG methods that conform to discontinuous material interfaces allow strong media changes to be modeled better, leading to more accurate simulations. One can also model the effects of attenuating material within the earth's interior with additional equations. However, these equations, along with the extremely large number of inversion parameters, create a tremendous burden on computational resources. Sandia is thus exploring new algorithmic approaches to help reduce these costs.

Traditionally, discontinuous material interfaces have been smoothed to allow easy meshing of the computational domain as well as compatibility with high-order finite-difference methods for modeling wave propagation. However, with Sandia's unstructured DG methods, these interfaces can be better represented, producing more accurate results (Figure 1 bottom). As noted above, seismic wave attenuation, where wave energy is absorbed and experiences changes in waveform amplitude and shape, is complex and costly to model. It is very important to include, however, and Figure 2 illustrates the difference between a simulation with (right) and without (left) attenuation. These differences would affect the estimated earth properties obtained through inversion, leading to a potentially misleading prediction of the earth's interior.

The cost of inversion is directly related to the number of inversion parameters. Many inverse problems for engineering applications have at most tens of parameters. However, for seismic inversion one needs to invert for billions of field parameters (*e.g.*, density and bulk modulus for acoustic inversion) producing a tremendous computational challenge.

Even with peta-scale computers, an inversion could take hundreds of CPU-days. An example acoustic inversion using the Sandia DG inversion tool is shown in Figure 3. The current work focuses on exploiting the flexibility of the DG method to further improve seismic inversion.

References

1. J. R. Krebs, J. E. Anderson, D. Hinkley, A. Baumstein, S. Lee, R. Neelamani, and M.D. Lacasse. Fast full wave seismic inversion using source encoding. SEG Technical Program Expanded Abstracts, 28(1): 2273–2277, 2009. doi: 10.1190/1.3255314. URL <http://link.aip.org/link/?SGA/28/2273/1>.
2. J. R. Krebs, J. E. Anderson, D. Hinkley, R. Neelamani, S. Lee, A. Baumstein, and M. D. Lacasse. Fast full wave seismic inversion using encoded sources. Geophysics, 74 (6): 177–188, 2009. doi: 10.1190/1.3230502.
3. G. S. Martin, R. Wiley, and K. J. Marfurt. Marmousi2: An Elastic Upgrade for Marmousi. The Leading Edge, 25:156–166, February 2006.

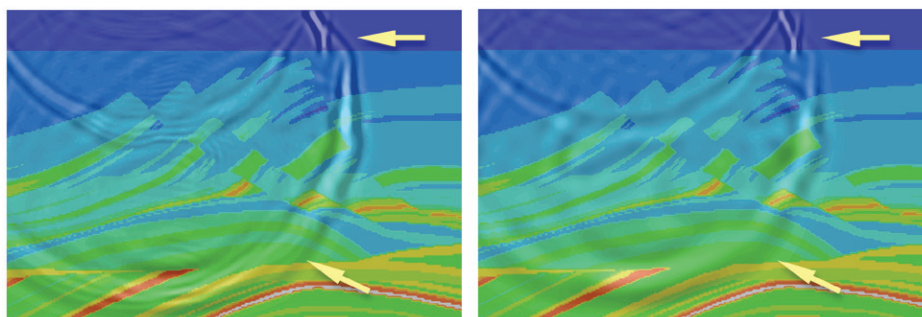


Figure 2: Simulated acoustic wave propagation without attenuation (left), and wave propagation with attenuation (right) through the Marmousi2 model.

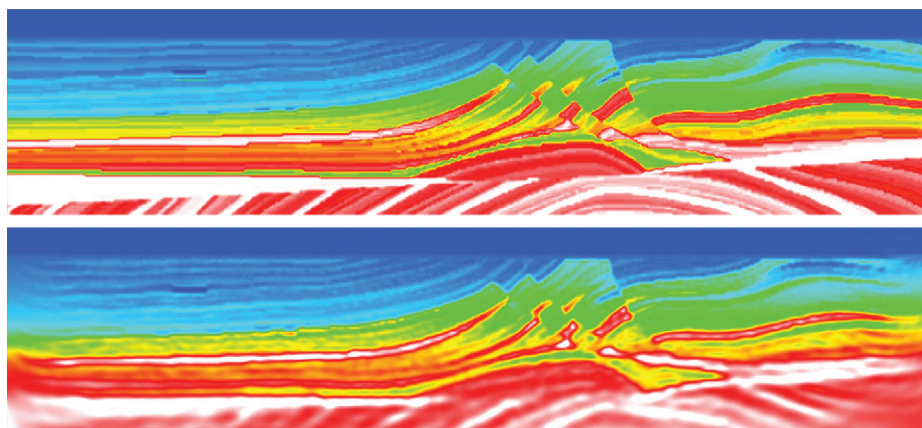


Figure 3: Inversion of the Marmousi2 model where the predicted sound-speed (bottom) is in good agreement with the true sound-speed (top). Conditions similar to those in Krebs et al. (References 1,2)

Computer and Information Sciences

Quantum Computing

To Protect Quantum Information, Understand What Threatens it

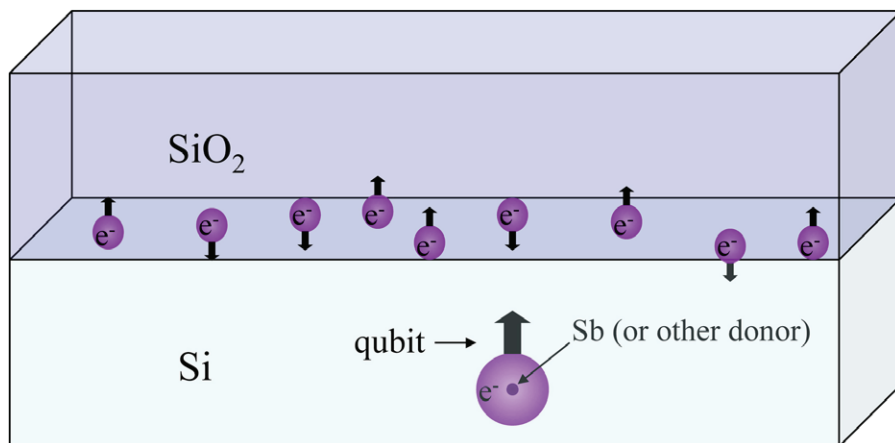


Figure 1: Decoherence of a donor qubit in silicon from a surface of electrons at random defect sites.

*Progress is being made
in understanding
how qubits lose their
information during
interactions with
system noise.*

For more information:

Technical Contact:

Wayne M. Witzel
505-844-8330
wwitzel@sandia.gov

Richard P. Muller
505-284-3669
rmuller@sandia.gov

Science Matters Contact:

Alan Burns
505-844-9642
aburns@sandia.gov

The famous physicist Richard Feynman surmised that a computer engineered to exploit quantum phenomenon (i.e., a quantum computer) could be vastly more powerful than a classical computer. However, the feasibility of building a quantum computer was not broadly accepted until Peter Shor discovered a means for quantum error correction despite the limitation that quantum information cannot be fully copied nor measured. Shor also devised a quantum algorithm for factoring integers that had an exponential improvement over the best-known classical algorithm, with important implications for cryptography and national security. Since then, dozens of quantum algorithms have been developed and quantum information theory has progressed sufficiently that it is now practical to address the engineering problem of building a quantum computer.

A primary problem for quantum computing is to devise practical physical means of storing quantum computational binary digits, or *qubits*. Any two-level quantum mechanical system can serve as a qubit. There are many proposed systems

involving states of photons, electrons, nuclei, atoms, or even superconducting circuits. A general problem is that the qubits must maintain their quantum information for usefully long periods of time (milliseconds), relative to the duration of logical gate operations. The culprit in the loss of qubit information, quantum decoherence, must be understood and minimized. For this reason, Sandia has developed computational methods to simulate potential sources of decoherence, and thus give guidance to how experimental qubit fabrication can best be improved.

At Sandia, an effort is underway to develop a qubit from the spin of a localized electron in a silicon crystal, either in an electrostatically-confined quantum dot or bound to a donor such as antimony (Sb, see Figure 1). Since this qubit must be sufficiently isolated to preserve its information for milliseconds, understanding decoherence in this system as a function of time is critically important. In particular, the electron spin is susceptible to magnetic fields from nuclear spins or other electron spins, which fluctuate due to interactions

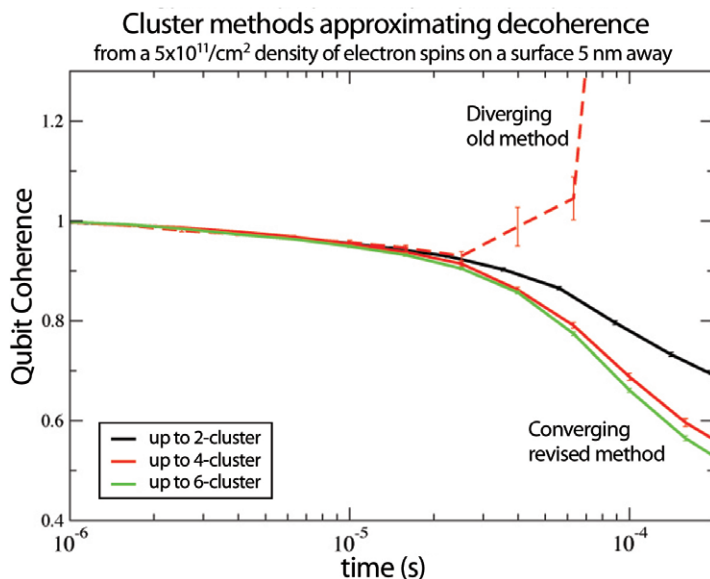


Figure 2: Revised cluster methods have made it possible to study problems of sparse electron spins baths.

with each other. Therefore, it is necessary to simulate the system of a spin qubit within a bath of many environmental spins interacting with each other through mutual magnetism. This presents the exponentially-scaling difficulty of simulating a quantum system.

Fortunately, one only needs to compute information about the initial coherence loss of the qubit. Processes involving two spins will occur before processes involving more spins, and the initial coherence loss can be analyzed very well using a mathematical cluster expansion that successively includes processes involving an increasing number of spins. In this way, the computation no longer scales exponentially with the size of the problem; rather, it scales exponentially with the required cluster size. The cluster expansion works particularly well for the problem of an electron spin that is strongly coupled to a large number of nuclear spins through direct contact (hyperfine) interactions. The nuclear spins have relatively weak magnetic interactions with each other, and a strong external magnetic field is applied. The full coherence decay can be well-approximated with clusters of only two spins (Reference 1). The cluster correlation expansion was later developed (Reference 2) to extend the method to the regimes of a sparse bath and is a cleaner formulation that is always exact in the large cluster limit.

The current research involves a sparse bath of electron spins where interactions with the qubit spin are no stronger than interactions among bath spins. In Reference 3, decoherence induced from spins of electrons bound to a background of phosphorus donors in bulk silicon is considered. An example is illustrated in Figure 1, where a surface of electrons at defects along an interface may induce decoherence of a qubit through their spin interactions. In these problems, larger clusters do play a more important role. This new regime also necessitates some revisions of the cluster correlation expansion formalism. In particular, good convergence is not achieved until one averages over the state of some of the spins that are external to a given cluster in a self-consistent manner; this stabilizes the random effects of a sparse bath (Figure 2). Sandia continues to extend these techniques in an effort to understand and then mitigate sources of decoherence that hinder progress on quantum computation.

References

1. W. M. Witzel, Decoherence and Dynamical Decoupling in Solid-State Spin Qubits, <http://hdl.handle.net/1903/6889> (dissertation, 2007); W. M. Witzel, R. de Sousa, S. Das Sarma, Quantum theory of spectral diffusion induced electron spin decoherence, *Phys. Rev B* **72**, 161306(R) (2005); W. M. Witzel, S. Das Sarma, Quantum theory for electron spin decoherence induced by nuclear spin dynamics in semiconductor quantum computer architectures: Spectral diffusion of localized electron spins in the nuclear solid-state environment, *Phys. Rev. B* **74**, 035322 (2006). W. M. Witzel and S. Das Sarma, Multiple-pulse coherence enhancement of solid state spin qubits, *Phys. Rev. Lett.* **98**, 077601 (2007).
2. Wen Yang and Ren-bao Liu, Quantum many-body theory of qubit decoherence in a finite-size spin bath, *Phys. Rev. B* **78**, 085315 (2008).
3. Wayne M. Witzel, Malcolm S. Carroll, Andrea Morello, Lukasz Cywinski, and S. Das Sarma, Electron spin decoherence in isotope-enriched silicon, arXiv:1008.2382.

Combustion Science Biofuels

Fundamentals of Biofuel Combustion Chemistry

As biofuels replace fossil fuels, the combustion chemistry must be optimized for tomorrow's engines.

For more information:

Technical Contact:

Nils Hansen
925-294-6272
nhansen@sandia.gov

Science Matters Contact:

Alan Burns
505-844-9642
aburns@sandia.gov

Currently, 85% of the world's energy demand is met by the combustion of fossil fuels. The critical consequences of future supply shortages and environmental degradation (climate change and air pollution) have motivated many nations to transition away from conventional fuel sources and to instead utilize biofuels such as bio-ethanol, bio-butanol, and biodiesel. Biofuels offer the advantage of coming from large, mainly under-utilized biomass resources that are sustainable and renewable in a closed carbon cycle that reduces environmental impact.

Biofuels are already being blended with gasoline and diesel fuel for automotive and heavy-duty ground transportation. However, in order for biofuel combustion technology to evolve towards greater efficiency and reduced formation of harmful pollutants, a molecular-level

description of the combustion processes is necessary. From a chemical point of view, the typical biomass-derived fuel (alcohols, ethers, or esters) contains oxygen in its molecular structure; whereas, conventional hydrocarbon fossil fuels typically contain only carbon and hydrogen. While decades of combustion research have been performed on hydrocarbon fuels, investigations of the richer combustion chemistry of the oxygenated biofuels have only just begun.

Scientists at Sandia's Combustion Research Facility (supported by the Dept. of Energy, Office of Basic Energy Sciences) have collaborated over the past several months with colleagues at Cornell University and the University of Bielefeld in Germany to provide new insights into the complex reaction pathways associated with the combustion of biofuels. In their experimental work, mass spectrometry and laser-based techniques

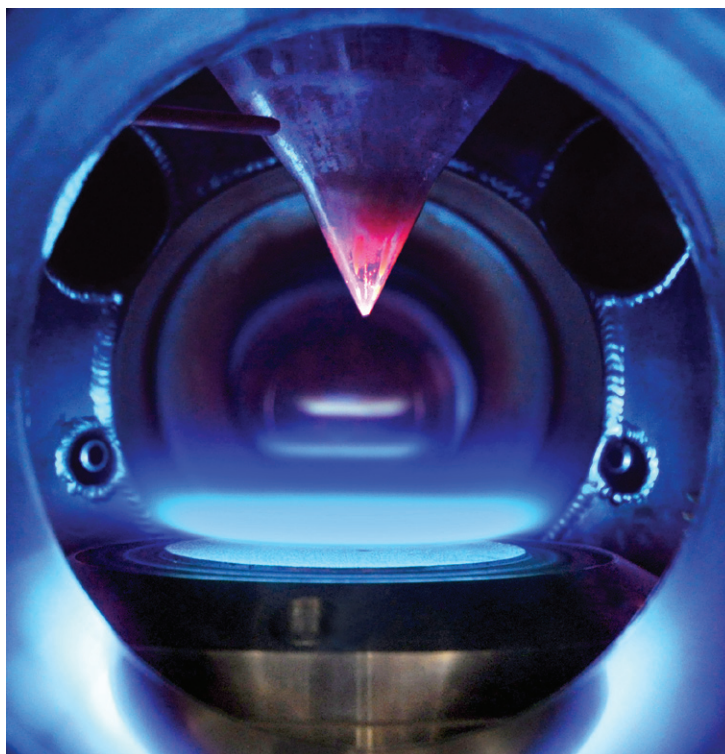



Figure 1: Flame analysis with photoionization molecular-beam mass spectrometry. Gases from a burner-stabilized flame (bottom) are sampled as a function of distance from the burner surface using a quartz cone (center), expanded into higher vacuum, and guided into the ionization chamber of a time-of-flight mass spectrometer for quantitative analysis.



are used to reveal the detailed chemical composition of laboratory-based model flames fueled by prototypical biofuel compounds. A photograph of such a model flame is shown in Figure 1. The flames are typically stabilized on a porous-plug burner at reduced pressure to widen the reaction zone where many of the intermediates are formed and consumed. Such a configuration ensures spatial homogeneity across the burner diameter and the combustion progress can be described in one dimension, i.e., as function of distance from the burner.

Exciting advances have been made possible in flame-sampling mass spectrometry experiments by employing tunable vacuum-ultraviolet photoionization at the Advanced Light Source (ALS) of Lawrence Berkeley National Laboratory (Reference 1). This sampling technique, combined with the mass spectrometric analysis, is the only viable detection method which provides selective and sensitive detection of all combustion intermediates simultaneously. Furthermore, the ALS-based experiment allows for the unambiguous detection of chemical compounds with the same empirical formula but different bond structures (i.e., isomers). Under identical conditions, isomers tend to react differently; therefore, isomer-resolving studies are of great value for the investigation of complex reactive environments as they yield a molecular-level description of the combustion chemistry. In order to develop such a step-by-step understanding of the entire combustion process, the experimental data sets are modeled using computer simulations in collaboration with Princeton University, North Carolina State University, and Lawrence Livermore National Laboratory.

In recent investigations, the influence of the chemical structure of biofuel molecules has been studied with respect to formation of intermediates and products, including pollutants. While the combustion chemistry of ethanol and dimethyl ether are relatively well understood, efforts are under way to unravel the important reaction steps in flames fueled by larger alcohols, such as propanol and butanol (Reference 2). From the results at hand, it might be inferred more generally that the combustion of oxygenated, bio-derived fuels would reduce the formation of soot and its precursors compared to the combustion of widely used fossil

fuels. Methods are also being developed to understand the mechanisms to describe the combustion chemistry of biodiesel fuels, which contain large methyl esters derived from a variety of vegetable oils and animal fats. However, largely because of the structural complexity of these large compounds, a molecular-level description of the respective combustion chemistry is still incomplete. Consequently, smaller, prototype methyl esters are being used as valuable steps towards a better understanding of the reaction pathways (Reference 2). The combustion chemistry of these small, prototypical methyl esters is not necessarily of direct practical relevance; however, any detailed combustion chemistry model describing their combustion behavior should be an important subset for predicting the combustion behavior of more realistic biodiesel compounds.

In conclusion, the chemical composition of transportation fuel is likely to change in the near future, with new biofuels already being established on the market. In order to make the most effective use of them, and to determine their emission characteristics, scientific research is under way to provide a detailed understanding of the underlying combustion chemistry.

References

1. N. Hansen, T. A. Cool, P.R. Westmoreland, K. Kohse-Höinghaus, Recent Contributions of Flame-Sampling Molecular-Beam Mass Spectrometry to a Fundamental Understanding of Combustion Chemistry, *Progr. Energy Combust. Sci.*, 2009, **35**, 168-191.
2. K. Kohse-Höinghaus, P. Oßwald, T.A. Cool, T. Kasper, N. Hansen, F. Qi, C. K. Westbrook, P. R. Westmoreland, Biofuel Combustion Chemistry: From Ethanol to Biodiesel, *Angew. Chem. Int. Ed.*, 2010, **49**, 3572-3597.

Engineering Sciences

Thermal Science

The Phoenix Series of Liquefied Natural Gas Pool Fires



Figure 1: LNG cargo carrier entering Boston harbor for offload.



Figure 2: Large scale LNG pool fire experimental site.

*Large-scale experiments
enable researchers to
examine big spills that would
occur from LNG tankers*

For more information:

Technical Contacts:

Thomas K. Blanchat
505-844-9061
tkblanc@sandia.gov

Michael M. Hightower
505-844-5499
mmhight@sandia.gov

Science Matters Contact:

Alan Burns
505-844-9642
aburns@sandia.gov

Due to the growing demand for natural gas nationwide, the number of liquefied natural gas (LNG) tanker deliveries to U.S. ports (Figure 1) is expected to increase, thus raising concerns about accidental spills or other events. The risks and hazards of a LNG spill will vary depending on its size, the environmental conditions, and the harbor. Risks include not only harm to nearby people, but also significant property damage and economic impact due to long-term interruptions in the LNG supply. Therefore, methods to ensure the security of LNG terminals and shipments in the event of an incident are critical from both public safety and property perspectives.

Much progress has been made in LNG threat consequence and vulnerability assessment. A general approach to risk evaluation has been developed, and is used as a basis in site-specific risk assessments. However, there are significant knowledge gaps in the science of very large-scale LNG pool fires. These gaps create serious uncertainties that may either under- or over-estimate latent hazards. Generally, the surface emissive power of a pool fire is a function of pool size and will increase

to reach a maximum value then decrease to reach a limiting value with increasing diameter. For LNG, the limiting power is uncertain. To fill the knowledge gaps and reduce uncertainty, it became necessary to leverage Sandia's considerable expertise in thermal science to stage very large (> 25-m diameter) LNG pool fires that would surpass by a factor of ten anything that had been attempted previously.

To accomplish this task, the Sandia team came up with a simple, low-cost concept of excavating a shallow 120-m diameter pool for the water, and then using the soil to create a deep, insulated 310,000 gallon reservoir to hold the LNG needed for the test (Figure 2). Concrete pipes from the center of the reservoir transported the LNG to the center of the water pool (Figure 3). A simple removable plug allowed gravity to control the flow rate (Figure 4). The considerable safety issues were reservoir integrity, thermal hazards (from cryogenic to extreme heat), asphyxiation, explosion, drowning, and aviation traffic. An advanced three-dimensional transport simulation was used to evaluate both the thermal performance of the reservoir and components, the

transport of gaseous boil-off during the cool-down process, and the design of the diffuser in the middle of the pool used to translate the linear momentum of the LNG in the pipes to a radially-spreading pool. Data was captured via cameras (gyroscopically stabilized and suspended from helicopters), spectroscopic diagnostics, and heat flux sensors.

Experiments were completed on two LNG spills, with diameters of 25 m and 85 m. Datasets will now allow model development and validation for extrapolation to a scale expected for a spill (300-500 m). The data had unexpected

results in that the fire diameter was smaller than the spreading LNG pool diameter (Figure 5). Previous studies with stagnant pools in pans had resulted in fires the same size as the pool. However, in all such studies, the pans have edges that can result in flame stabilization that would not be available on the open water. The data further showed that, in both very light and significant cross-winds, the flame will stabilize on objects projecting out of the water, suggesting that the ship itself will act as a flame holder.

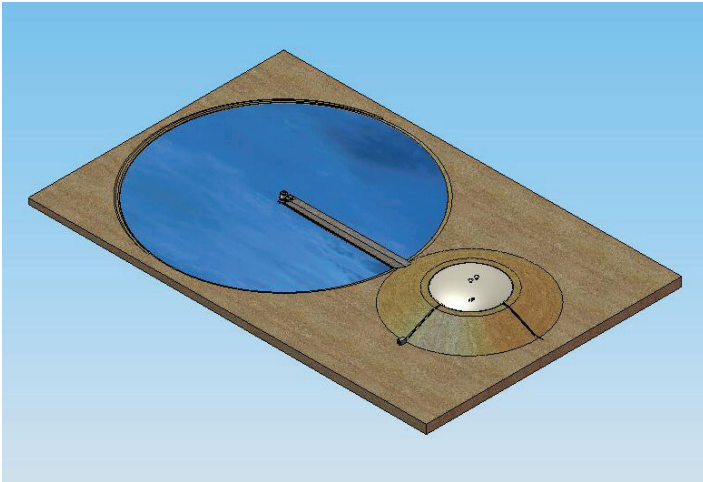


Figure 3: Schematic of test facility showing LNG reservoir (right), and concrete piping going to the center of the pool.

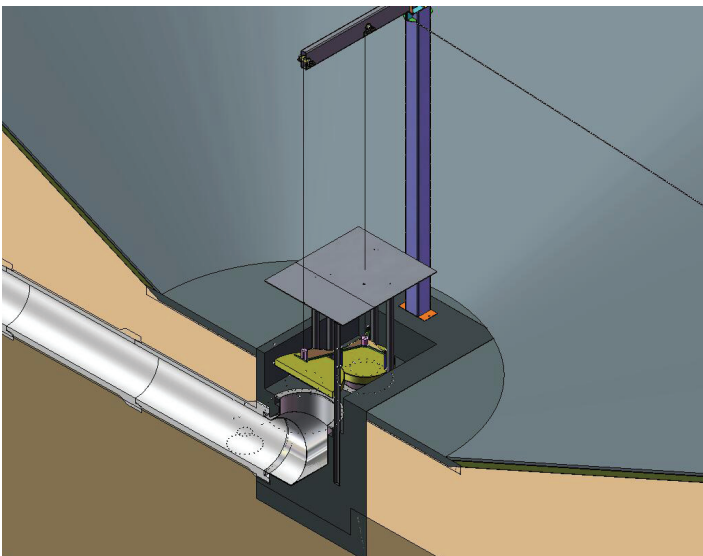


Figure 4: Schematic of gravity fed flow and removable plug in center of pool.



Figure 5: Image of 85-m pool fire that shows flames not extending across spreading (white area) LNG pool.

Engineering Sciences Thermal, Fluid and Aerosciences

Quantum-Kinetic Approach for Modeling Non-Equilibrium Gas-Phase Chemical Reaction Rates

*Progress is being made
in modeling reacting
gas flows under extreme
conditions, such as
vehicle re-entry.*

For more information:

Technical Contacts:

Michael A. Gallis
505-844-7639
magalli@sandia.gov

Ryan B. Bond
505-844-1891
rbbond@sandia.gov

John R. Torczynski
505-845-8991
jrtorc@sandia.gov

Science Matters Contact:

Alan Burns
505-844-9642
aburns@sandia.gov

In many technologically important areas involving reactive gas flows, including hypersonic reentry, materials processing, and microsystems, the gas is not in thermal equilibrium and cannot be characterized by a single temperature T . Thus, traditional chemistry models based on equilibrium (single-temperature) Arrhenius rates $k(T)$ cannot be used to accurately model non-equilibrium problems. The challenges of modeling non-equilibrium gas-phase chemical reactions are exemplified by hypersonic reentry into the earth's atmosphere (Figure 1) and other planetary atmospheres. For instance, nitrogen, which behaves as an inert gas in many processes, becomes chemically active under the high-temperature conditions of hypersonic reentry (~10,000 degrees). Atmospheric chemical reactions during hypersonic reentry are dominated by dissociation of molecular species and exchange reactions involving diatomic molecules and single

atoms. Ionization may also occur at higher temperatures.

Modeling chemical reactions at the extreme conditions of upper-atmosphere hypersonic flow has been very important from the Apollo era to the present because heat-absorbing endothermic chemical reactions can reduce heat transfer to the spacecraft. However, an in-depth understanding of the physical and chemical processes that take place in the flow field still remains elusive. The main reason for this is the difficulty in accurately measuring internal-energy-state-specific chemical reaction rates to validate theoretical models in the temperature range of interest. To avoid the inaccuracy of empirical Arrhenius-type chemical-reaction rates, new methods are being developed. The Direct Simulation Monte Carlo (DSMC) method of Bird (Reference 1), a molecular-gas-dynamics technique that tracks individual molecules as they move and collide, simulates gas flows

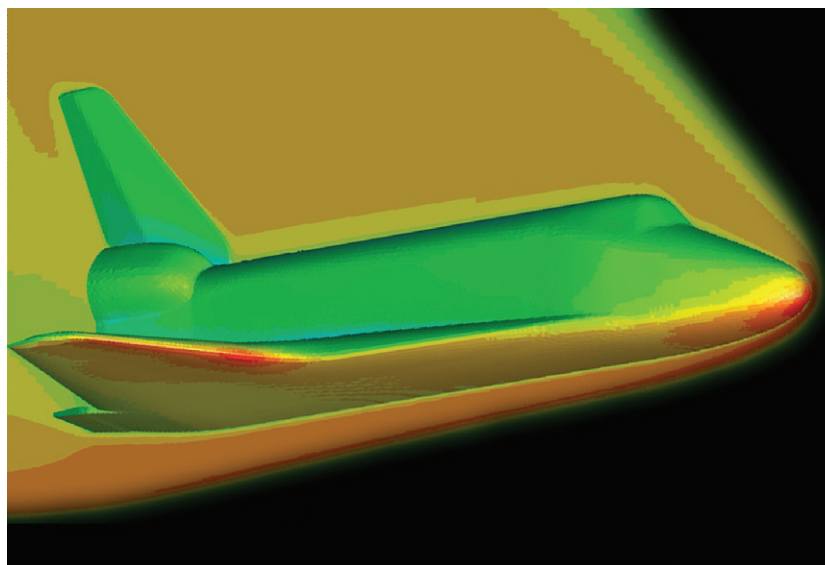


Figure 1: Simulation of the heating on the Space Shuttle as it enters the earth's atmosphere.

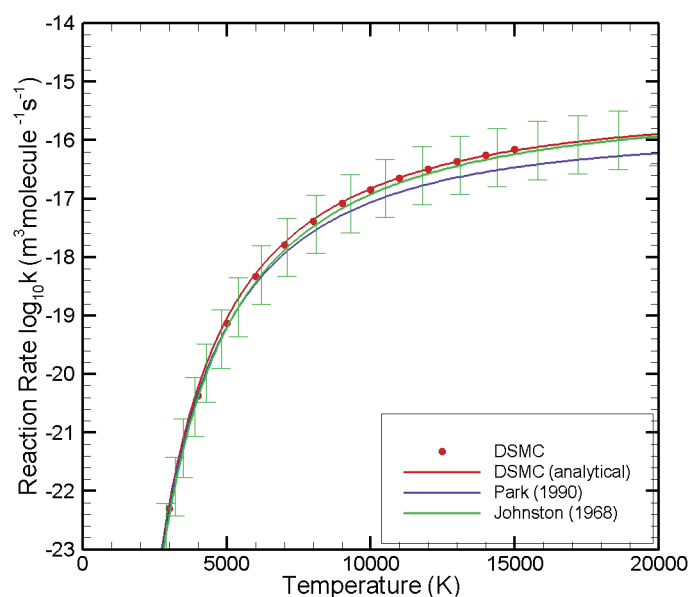


Figure 2: Comparison between predicted and measured equilibrium reaction rates for oxygen dissociation.

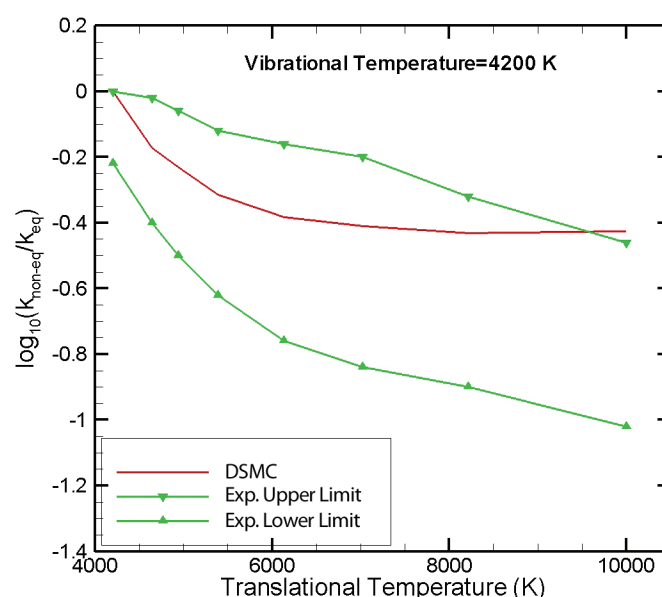


Figure 3: Comparison between predicted and measured non-equilibrium reaction rates for oxygen dissociation.

at the molecular level using kinetic-theory considerations and thus treats non-equilibrium gas behavior accurately. DSMC treats molecular collisions using stochastic rather than deterministic procedures to achieve greater computational efficiency.

Bird recently proposed a set of molecular-level “quantum-kinetic” chemistry models based solely on fundamental properties of two colliding molecules: their total collision energy, their quantized vibrational energy levels, and their molecular dissociation energies. These models link chemical-reaction cross-sections to the energy-exchange process and the probability of transition between vibrational energy states. These models apply directly to dissociation and endothermic exchange reactions. The energy-exchange procedures and the principle of microscopic reversibility are then used to derive models for the reverse situations: recombination and exothermic exchange reactions. These models do not require any macroscopic rate information, and they function by balancing the fluxes into and out of each state, thus satisfying microscopic reversibility.

At Sandia (References 2,3), this set of models was extended and refined for the dissociation of molecular oxygen under equilibrium (Figure 2) and non-equilibrium (Figure 3) conditions, and the resulting reaction rates are in good agreement with the best available measured or extrapolated reaction data. The experimental uncertainty of the measurements, typically one order of magnitude or greater, and the idealizations of the models do not allow

for an unequivocal assessment through these comparisons. However, the reaction-rate data and the DSMC predictions are always within one order of magnitude. This level of agreement is a source of optimism concerning the ability of the models to predict non-equilibrium reaction rates.

One of the most important features of this type of model is that it models chemically reacting flows from first principles, not only without knowledge of the macroscopic reaction rates but also without prior knowledge of which reactions will occur. As a result of their generality and flexibility, these models are currently being evaluated for reactions involving combustion, plasmas, complex molecules, and entry into other planetary atmospheres.

References

1. Bird, G. A., *Molecular Gas Dynamics and the Direct Simulation of Gas Flows*, Oxford University Press, Oxford, 1994.
2. Gallis, M. A., Bond, R. B., and Torczynski, J. R., A Kinetic-Theory Approach for Computing Chemical-Reaction Rates in Upper-Atmosphere Hypersonic Flows, *Journal of Chemical Physics*, **131**, 124311, 2009.
3. Gallis, M. A., Bond, R. B., and Torczynski, J. R., Assessment of Collision-Energy-Based Models for Atmospheric-Species Reactions in Hypersonic Flows, *Journal of Thermophysics and Heat Transfer*, **24**, 241-253, 2010.

Engineering Sciences

Accelerometers

Vibration-Induced Gas-Liquid Effects in Accelerometers

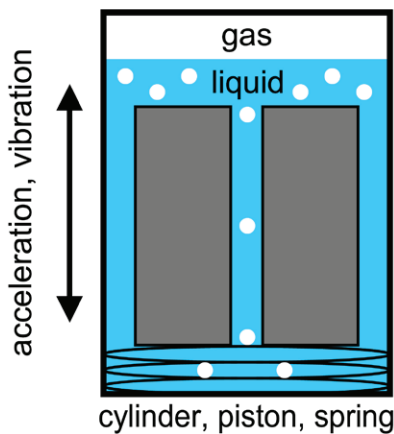


Figure 1: Schematic diagram of a liquid-filled mechanical accelerometer.

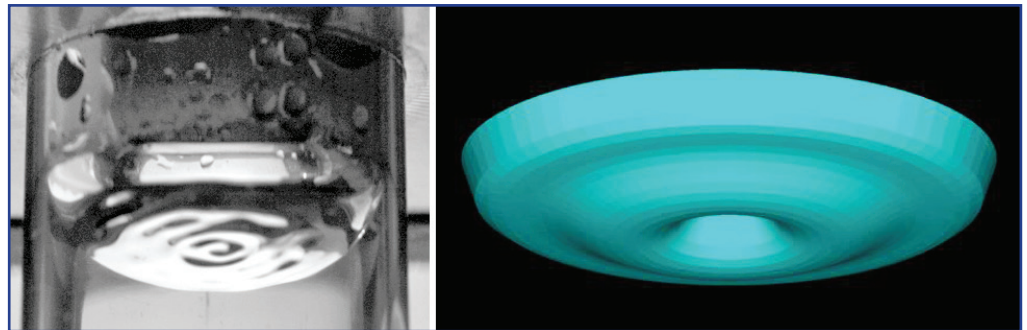


Figure 2: Vertically vibrating gas-liquid interface viewed from below. Left: Experiment where the liquid is contained in clear plastic cylinder and concentric waves appear on the bright circular free surface. Right: computer simulation.

Gas-liquid interactions in accelerometers experiencing vertical vibration can produce rich dynamical behavior.

For more information:

Technical Contacts:

Timothy J. O'Hern,
505-844-9061
tjohern@sandia.gov

John R. Torczynski
505-845-8991
jrtorc@sandia.gov

Science Matters Contact:

Alan Burns
505-844-9642
aburns@sandia.gov

Sensing acceleration accurately is essential to Sandia's nuclear weapons mission. Accelerometers for these applications are typically mechanical rather than electronic and must function reliably when subjected to intense vibration environments (Figure 1). During vibration, the gas and liquid in accelerometers can interact to produce waves (see Figure 2) and bubbles that impact the accelerometer's dynamical behavior.

A mechanical accelerometer has several internal components that affect its dynamics (Figure 1). The *cylinder* is a closed housing that actually experiences the applied acceleration and vibration. The *piston* is a massive solid object that moves along the cylinder's axis in response to the applied acceleration. The *spring* prevents the piston from moving downward until gravity plus acceleration exceed the spring's preload force. The *liquid* is a viscous oil that is forced upward through the piston's flow passages as the piston moves downward, thereby damping the motion. The *gas* is mostly air and partly oil vapor and is included to account for the different thermal expansion of the liquid relative to the solid components

over the intended temperature range. Although not shown, *electrical contacts* produce friction, which also damps the piston motion.

Under certain conditions of vibration, the interaction of these components can cause the piston to move downward against the spring even when the spring is more than strong enough to support the piston in the absence of vibration. This unexpected dynamical behavior is related to the transport of gas from the headspace above the piston to the spring region below the piston. Anomalous piston motion has been conjectured to consist of four steps: (1) generation of waves on the gas-liquid interface; (2) production of bubbles by these surface waves; (3) the (counterintuitive) downward net motion of these bubbles; and (4) the downward net motion of the piston, which is caused by the gas distributions created by these downwardly moving bubbles.

Theoretical, computational, and experimental investigations are underway to understand each of these steps and how they combine to cause anomalous piston motion. The major focus has been the

vibration-induced generation and growth of waves on the gas-oil interface (References 1,2). In 1831, the famous British scientist Michael Faraday showed that waves form on a gas-liquid interface when the liquid layer is vibrated vertically at certain frequencies and amplitudes. This parametric wave instability, known technically as a period-doubling bifurcation, has been studied in the past for thin layers of low-viscosity liquids like water.

Figure 3 shows the results of the present theoretical and computational investigations for large depths of a high-viscosity oil. For a given vibration amplitude (254 microns), waves occur only within certain frequency bands (e.g., 18.5-20.7 Hz), with more waves observed as the frequency is increased. The theoretical and computational predictions for these instability bands are in excellent agreement, typically to within 0.1 Hz. Figure 4 shows similar experimental results in which the displacement amplitude is held constant at 250 microns while the frequency is increased from 120 Hz to 160 Hz. In accord with theory, the waves increase in number and strength as the frequency is increased. The experiments reveal additional features not yet investigated theoretically or computationally, namely long thin liquid jets, droplets formed by these jets pinching off, and cavities formed by these droplets impacting the gas-liquid interface (see Figure 5). Computations to investigate these additional flow features are underway.

Future efforts will focus on making more detailed comparisons between the experiments and the theoretical results for wave generation and the other three steps in the conjectured route to anomalous piston motion in accelerometers. Of particular interest is how strong vibrations can induce downward bubble motion and stabilize a gas pocket below the piston. Two gas pockets, one above the piston and the other below it, can act together as an extra spring that enhances the downward motions of the gas and the piston. The long-term goal of this investigation is a quantitative, predictive understanding of each step in this process and how these steps work together to produce anomalous piston motion in accelerometers.

References

1. A. M. Kraynik, L. Romero, J. R. Torczynski, C. F. Brooks, T. J. O'Hern, R. A. Jepsen, and G. L. Benavides, "The Effect of Dynamic Wetting on the Stability of a Gas-Liquid Interface Subjected to Vertical Oscillations," *Bulletin of the American Physical Society*, **54** (19), p. 48 (2009).
2. L. Romero, J. R. Torczynski, and A. M. Kraynik, "A Scaling Law near the Primary Resonance of the Quasi-Periodic Mathieu Equation," *Nonlinear Dynamics*, submitted in April (2010).

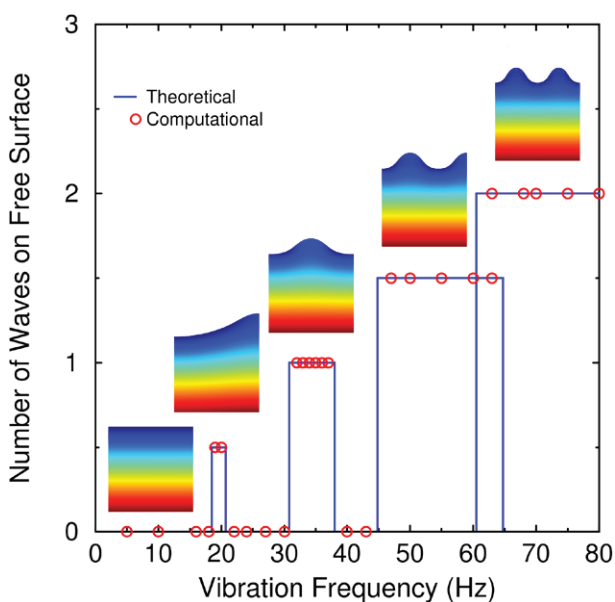


Figure 3: Number of waves on vertically vibrated gas-liquid interface.

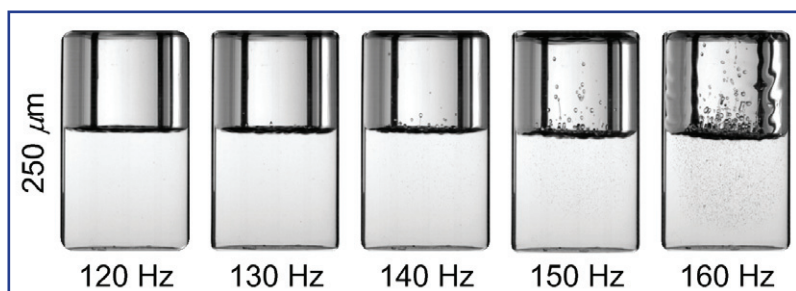


Figure 4: Increasing the frequency at fixed stroke increases the disturbance level.



Figure 5: Enlarged view of 160 Hz data in Fig. 4

Engineering Sciences Structural Mechanics

Coupled Multi-Physics Modeling to Support Energy R&D

Physical and chemical processes due to the burial of high-level radioactive waste can be simulated in greater detail with new engineering codes.

For more information:

Technical Contacts:

Mike Stone
505-844-5113
cmstone@sandia.gov

Mario J. Martinez
505-844-8729
mjmarti@sandia.gov

Science Matters Contact:

Alan Burns
505-844-9642
aburns@sandia.gov

Geologic repositories have played a critical role in US energy policy for several decades. The recent expansion of the Strategic Petroleum Reserve and the on-going operation of the Waste Isolation Pilot Plant to permanently dispose of low-level radioactive waste are prime examples of successful engineering of geologic systems to address critical national needs. These successes have fueled interest in developing other geologic systems for more challenging national energy problems, including high level nuclear waste disposal (Figure 1), compressed air methods for retrievable energy storage, utilizing geothermal energy, and CO₂ sequestration.

Development of long-term solutions to these needs requires the ability to model, simulate, and predict behavior of subsurface systems over geologic time scales. These behaviors include complex, heterogeneous mineral and porous rock thermo-chemo-mechanical behavior as well as the inter-

actions with multi-phase pore fluids and microbial activity. Recent investments by Sandia in the SIERRA Mechanics code suite provide the basic building blocks for realizing this multi-physics capability for geosystems engineering: fluid flow, nonlinear geomechanics, geochemistry, heat transfer, etc., with an application focus on CO₂ sequestration and radioactive waste disposal. This research has benefitted from collaborations with the University of Texas at Austin Center for Subsurface Modeling, and from interactions with the Center for Frontiers of Subsurface Energy Security which is an Office of Basic Energy Sciences Energy Frontier Research Center.

Here is shown how this modeling was recently applied in a feasibility analysis of high-level radioactive waste disposal in a clay/shale medium. A three-dimensional analysis of a section of a clay/shale waste repository is shown in Figure 1. The waste is stored in an unlined horizontal borehole

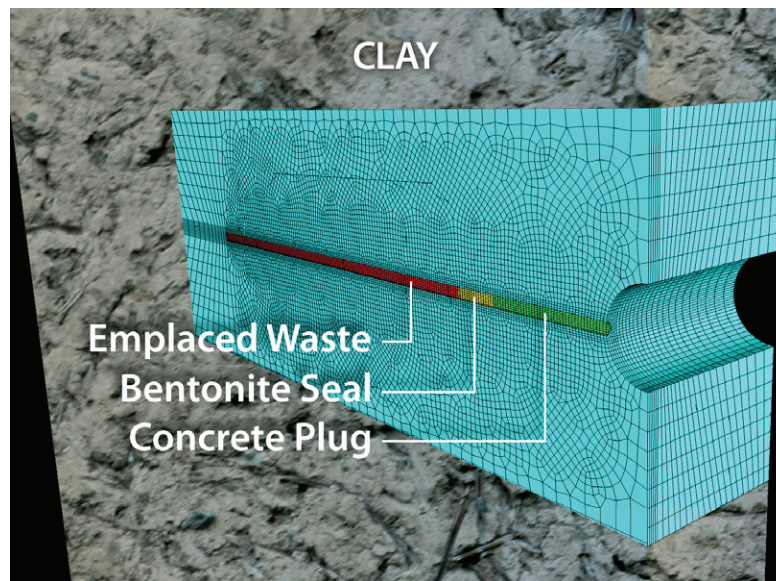


Figure 1: Clay/shale waste repository geometry with the finite element discretization showing the location of the emplaced waste, concrete, and bentonite plug.

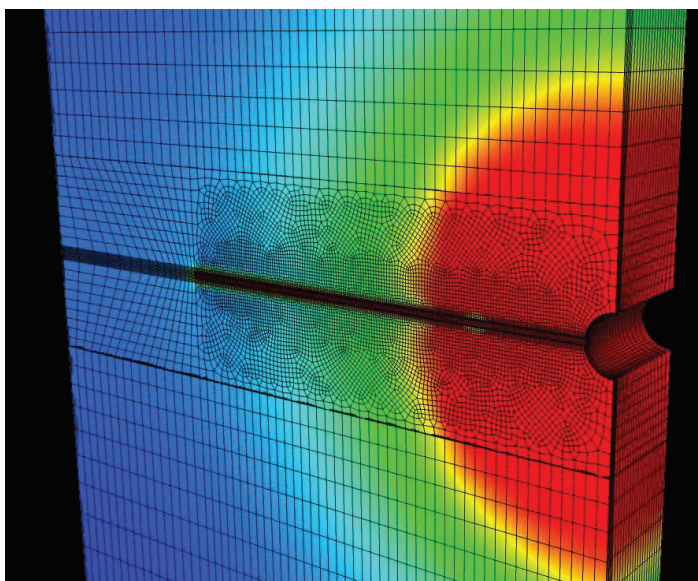


Figure 2: Region of assumed damage in the clay/shale after excavation. Red is a region of highest damage.

perpendicular to the main access tunnel. The disposal borehole would be sealed at the end with concrete and bentonite (a form of clay) plugs. The multi-physics approach was needed due to a coupling between the high heat generated by the radioactive waste, the presence of water, and the dependence of clay/shale strength and deformability

on the water content. Moreover, since thermally-driven fluid movement may transport radionuclides away from the waste source, species transport was included in the analysis.

Figure 2 shows the region of damage that results due to the initial excavation of the access tunnel and borehole, where red indicates a possible increase in local clay/shale porosity and permeability. Fractures and voids that form during excavation will eventually heal over time due to the sealing nature of the clay. However, peak emplacement borehole temperatures can range from 83 °C for typical high-level waste power densities to greater than 200 °C for some very high-level wastes. The simulation shows that the heat results in water evaporation in the repository near the emplacement boreholes (Figure 3). The extent of dessication also depends strongly on ambient rock permeability and, in some clays, will persist for a few thousand years. In contrast, high temperatures in combination with ultra-low rock permeabilities can trap high pressure superheated water vapor, potentially damaging the repository.

It has been shown in this waste repository example that the multiphysics capability in SIERRA Mechanics can model first-order interactions between important thermal, hydrological, and chemical processes. The development of the modeling capability has provided Sandia's scientists and engineers a new tool for modeling complex subsurface behavior and is currently being used to address other important areas of energy research such as CO₂ sequestration.

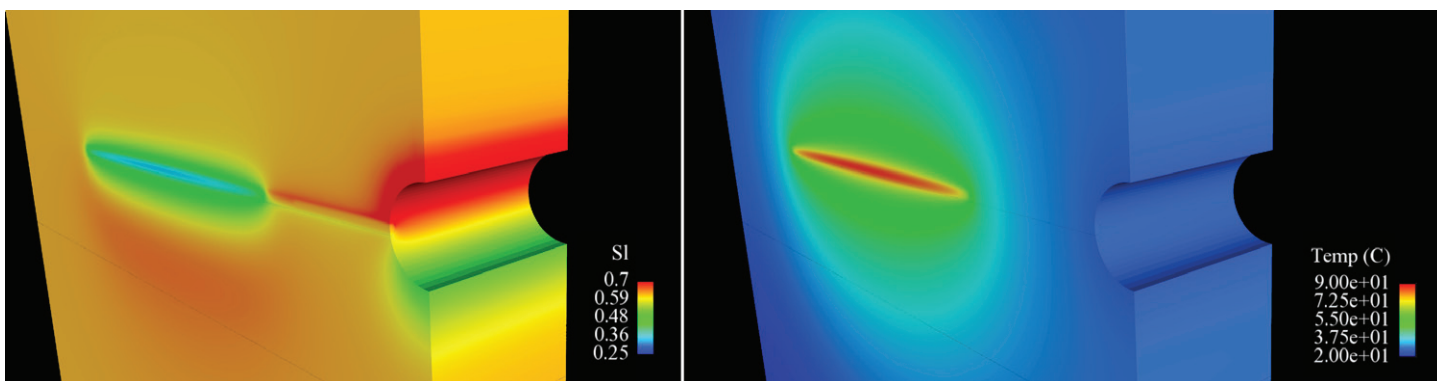


Figure 3: Water saturation (left) and temperature (right) contours near the waste horizon. Radioactive waste with high thermal output can produce dry out regions.

Material Science and Technology

Computational Materials Science

How Grain Growth Stops: A New Solution to an Old Mystery

Controlling grain size is a fundamental problem in materials science with technological implications.

For more information:

Technical Contacts:

Elizabeth A. Holm
505-844-7669
eaholm@sandia.gov

Stephen M. Foiles
505-844-7064
foiles@sandia.gov

Science Matters Contact:

Alan Burns
505-844-9642
aburns@sandia.gov

Most metals and ceramics are polycrystalline; they are comprised of many individual crystallites, called grains. The sizes, shapes and arrangement of these grains are important to the properties of the material – sometimes more important than the chemical composition. Understanding and controlling grain structure is important to nearly every engineered material. For materials that rely on strength, such as structural steel, a very fine grain size is desirable. On the other hand, there are important systems, such as silicon photovoltaics (Figure 1), in which a large, or even single crystal, grain size is preferred. Because the grain structure governs how a material performs, materials scientists have studied how to manipulate it for nearly two centuries. However, there are limits to how far the grain structure can be modified. For example, it is very difficult to create extremely small or large grains. While the lower limit of grain size is well understood – it is set by the atomic scale – the upper limit of grain size remains a mystery. Why can't grains grow beyond a certain size?

Grains are separated by interfaces called grain boundaries. Because atomic bonds are broken at grain boundaries, they contribute energy to the system. That implies that the lowest energy state of the system should contain no grain boundaries; in other words, the equilibrium state of most metals and ceramics should be a single crystal. When polycrystalline materials are heated to sufficiently high temperatures, the grain boundaries move and rearrange so as to decrease the amount of grain boundary present. However, even at very high temperatures and very long times, grain growth rarely proceeds to the single crystal state. Instead, grain growth nearly always stops even though many grains remain. Why grain growth stops is one of the oldest, most fundamental questions in materials science. It's not a purely academic question, either. It is challenging and expensive to make single crystals and usually depends on careful melt processing. If one could create single crystal silicon photocells by a solid-state process, the cost of solar panels would drastically decrease.

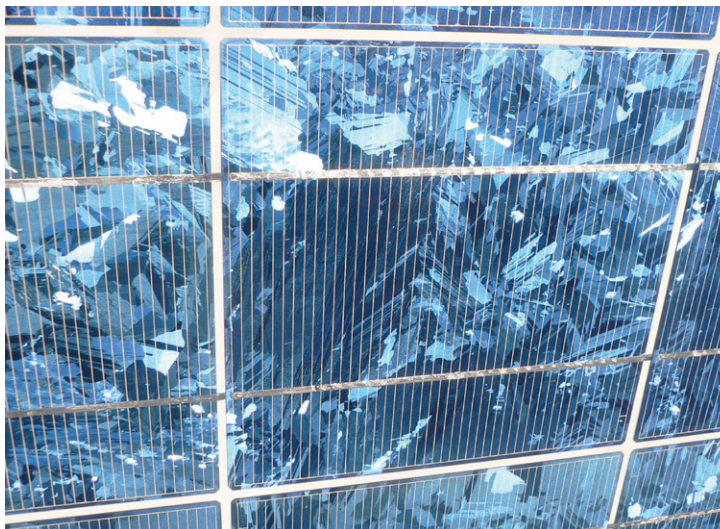


Figure 1: Stagnant grain structures in high-purity silicon photocells; single crystal photocells would be more efficient, but cannot be made by grain growth processing due to grain stagnation.

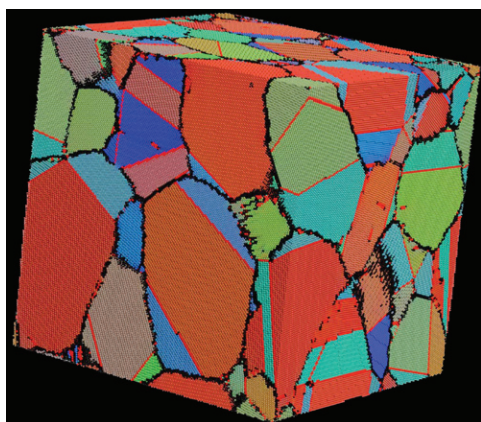


Figure 2: A stagnating grain structure in pure nickel, simulated on the atomic scale. Individual atoms are colored according to their grain membership, with black atoms denoting grain boundaries. Even though grain growth has slowed dramatically, many grains remain, and the structure is far from the equilibrium single crystal state. Previous grain growth models cannot explain the stagnation phenomenon.

There have been many mechanisms proposed for grain growth stagnation, each valid for certain materials and processes. However, none of these mechanisms has been able to explain grain growth stagnation for an important class of materials that includes photovoltaics: polycrystalline materials of very high purity.

At Sandia, a new mechanism has recently been discovered for grain growth stagnation that has not been described, or even speculated upon, before (Reference 1). This insight was enabled by the combination of atomistic and grain-scale simulation and illustrates the power of computational modeling to reveal physical phenomena unattainable by other methods. In recent large-scale simulations of several hundred individual grain boundaries, it was discovered that grain boundaries can be separated into two classes – fast and slow moving– depending on their atomic structure (References 2,3). The proportion of fast and slow boundaries depends on the temperature of the system. A grain-scale simulation was used to determine how the fast/slow ratio changes grain growth when many grains are present. It was found that when all boundaries are fast, growth proceeds to the equilibrium single crystal state. In contrast, if any slow boundaries are present, grain growth stops short of the single crystal, with the fraction of slow boundaries determining how many grains remain – even when the material is perfectly pure.

Because pure materials are hard to come by in the real world, confirmation of the discovery was obtained by using atomistic simulation techniques to build a pure polycrystal from the atoms up. A grain structure was thus constructed containing several hundred interconnected grains and heated to various temperatures. Figure 2 shows the result: Grain size grows at early times, but then slows short of the single crystal state, with the final structure containing many individual grains.

The size of the remaining grains is in good agreement with the predictions of grain-scale simulations, as shown in Figure 3. Although this is not conclusive proof that slow boundaries stop grain growth, it is highly suggestive – and no other stagnation mechanism is known in perfectly pure polycrystals.

Because controlling grain size to optimize properties is a fundamental problem in materials science, understanding how grain growth stops is a centuries-old problem. While a number of mechanisms have been proposed, slow grain boundary stagnation is the first new stagnation mechanism proposed in half a century and the only one to explain how grain growth stops in perfectly pure materials. With this new insight, materials scientists can begin to understand – and hopefully control – grain growth stagnation in important classes of engineered materials.

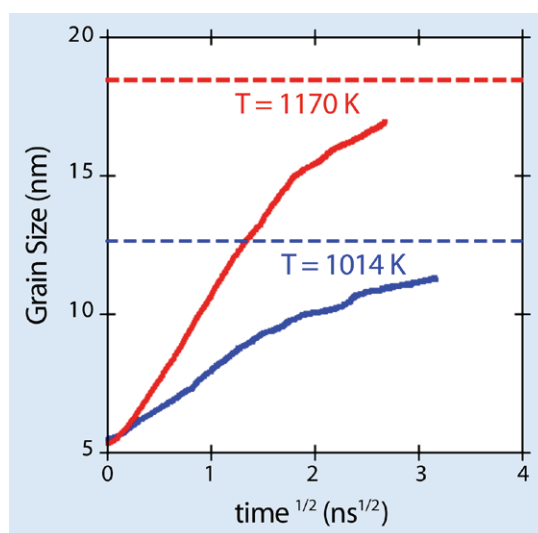


Figure 3: In atomic-scale simulations at two different temperatures, grain size increases for a while and then slows dramatically at later times, as shown by the solid lines. The grain size at stagnation agrees well with the predictions of a grain-scale model based on slow boundaries, shown as dashed lines. This agreement suggests that slow boundaries can stop grain growth even in perfectly pure materials.

References

1. Holm, E.A. and S.M. Foiles, How Grain Growth Stops: A Mechanism for Grain-Growth Stagnation in Pure Materials. *Science*, 2010. **328**(5982): p. 1138-1141.
2. Olmsted, D., S.M. Foiles, and E.A. Holm, Survey of computed grain boundary properties in face-centered cubic metals: I. Grain boundary energy. *Acta Materialia*, 2009. **57**(13): p. 3694-3703.
3. Olmsted, D., E. Holm, and S. Foiles, Survey of computed grain boundary properties in face-centered cubic metals-II: Grain boundary mobility. *Acta Materialia*, 2009. **57**(13): p. 3704-3713.

Materials Science and Technology

Organic Materials

Removable Encapsulants

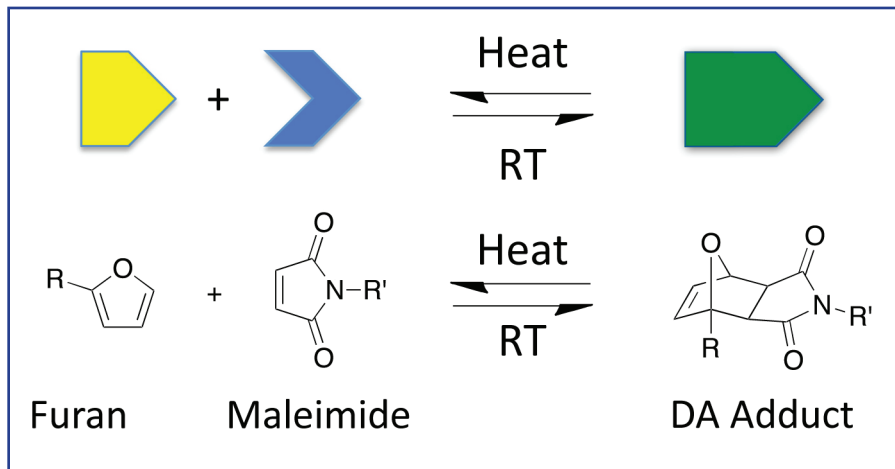


Figure 1: Reversible Diels Alder reaction
(RT= room temperature)

*Engineers are now able to
access critical engineered
system assemblies without
risk of damage*

For more information:

Technical Contacts:

James R. McElhanon
505-844-9165
jrmcelh@sandia.gov

Edward M. Russick
505-844-4357
emrussi@sandia.gov

James H. Aubert
505-844-4481
jhauber@sandia.gov

Science Matters Contact:

Alan Burns
505-844-9642
aburns@sandia.gov

Encapsulant foam materials have been used for decades in electromechanical assemblies for shock and vibration mitigation, structural support, and high voltage containment. In order to rework or repair the delicate assemblies, engineers have to gingerly remove the pervasive encapsulants without causing component damage. Current methods of traditional encapsulant foam removal involve the use of mechanical picking with tools, chemical removal with aggressive solvents, or media blasting, all which are known to damage or destroy printed wiring boards, plastics, and wiring interconnects. Easy encapsulant removal without damage to components is thus highly desirable and will become even more critical for engineering assemblies that must be in service for a long lifetime. To meet this need, Sandia has developed a suite of thermally-removable encapsulant foams.

The easily removable encapsulants are based on the well-known Diels-Alder (DA) chemical reaction (Figure 1). One variant of the DA reaction is the thermally-reversible [4 + 2] cyclo-addition between furan and maleimide molecules. Simply mixing the two species together at room temperature will cause the reactants to form a DA adduct.

Heating the adduct to temperatures greater than 50 °C, in the presence of a solvent, will induce the retro-DA reaction, which reverts the DA adduct back to the furan and maleimide starting materials. Under the correct conditions, the process is completely reversible and can occur over and over again without degradation to the starting materials.

Sandia has implemented these thermally-removable encapsulants into engineered systems in four different products: 1) REF308 removable epoxy foam, 2) REF320 removable epoxy foam, 3) RSF200 removable syntactic foam, and 4) RCC removable conformal coating. Each of the encapsulants utilizes a bis-epoxy DA resin that can undergo standard amine-epoxy curing reactions. Under normal operating conditions, the cured removable materials behave like typical encapsulants. They can be removed by placing the entire assembly in a stirred bath of furfuryl alcohol, a solvent derived from corn cobs, at a temperature of 50 °C. Under the conditions of elevated temperature and solvent, the reversion of the DA adducts back to their starting materials causes the encapsulants to covalently disassemble, dissolve, and be

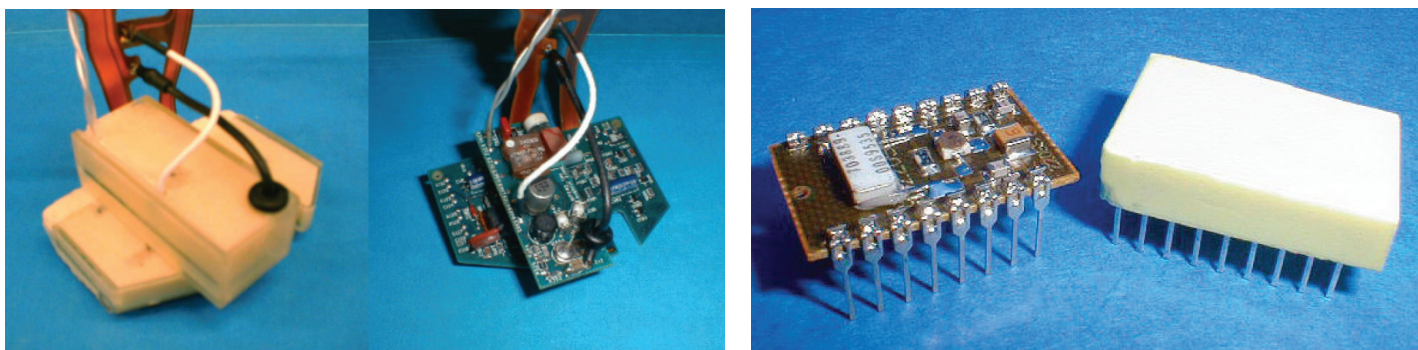


Figure 2: Foam and encapsulant removal: (left) removable epoxy foam (REF), (right) removable syntactic foam (RSF).

removed from the assembly (Figure 2). Furfuryl alcohol at 50 °C has been shown to be relatively harmless to mechanical and electrical components.

The removal mechanism incorporated into the materials by the addition of DA adducts provides a novel capability to perform repair, replacement, and surveillance of engineered systems that had not been available with conventional polymeric encapsulants. In particular, the ability to perform surveillance on encapsulated systems that require a long service lifetime is extremely valuable in assessing aging and reliability of high-value electromechanical systems. Through this work, Sandia has spawned new areas of research and has developed several other products using thermally-reversible DA reactions. These include thermally-reversible, covalent, self-assembling dendrimers, polymeric macromolecules, and cleavable surfactants (References).

References

1. Polaske, N.W; McGrath, D.V.; McElhanon, J.R. *Macromolecules* 2010, **43**, 1270-1276.
2. Szalai, M.L; McGrath, D.V.; Wheeler, D.R.; Zifer, T.; McElhanon, J.R. *Macromolecules* 2007, **40**, 818-823.
3. McElhanon, J.R. et. al. *Langmuir* 2005, **21**, 3259-3266.
4. McElhanon, J.R.; Russick, E.M.; Wheeler, D.R. Loy, D.A.; Aubert, J.H. *J. Appl. Polym. Sci. Chem. Soc.* 2002, **85**, 1496-1502.
5. McElhanon, J.R; Wheeler, D.R. *Org. Lett.* 2001, **3**, 2681-2683.

Material Science and Technology

Nanoscience

The Role of Carbon Surface Diffusion on the Growth of Epitaxial Graphene on SiC

Graphene monolayers hold considerable promise in nanoscale electronics if the growth mechanisms can be controlled.

For more information:

Technical Contacts:

Taisuke Ohta
505-284-3167
tohta@sandia.gov

Norman C. Bartelt
925-294-3061
bartelt@sandia.gov

Science Matters Contact:

Alan Burns
505-844-9642
aburns@sandia.gov

Graphene is the thinnest material ever known. It is a single atomic layer of carbon (graphite), and because of its excellent electronic, thermal, and mechanical properties, there has been considerable research concerning applications in nanoscale electronics. One of the biggest challenges in developing graphene-based electronics is how to synthesize it. Furthermore, to be useful in nanoelectronics, the synthesis method has to be scalable to produce graphene films the size of standard semiconductor wafers, at least a few inches in diameter. In general, good quality carbon-based materials are produced in high-temperature or high-pressure environments. These harsh environments restrict the options of material synthesis, and limit a deeper understanding of growth processes. Thus controlling growth of a one-atom-thick film over square-inches of area presents many challenges.

Graphene growth on a silicon carbide (SiC) substrate is regarded as one of the

promising ways to achieve graphene-based electronics. When SiC is heated, sublimation of Si takes place, leaving behind carbon atoms which assemble (“graphitize”) into graphene layers. Recently, it was found that heating SiC in argon at atmospheric pressure leads to significant improvements in size, film thickness, and electronic properties compared to heating SiC in vacuum. However, to gain better control and to further improve the quality of the graphene films, a comprehensive understanding of the growth processes and kinetic pathways is needed.

Using various microscopy techniques, researchers at Sandia have studied the transient stage when the first graphene layer is growing. Figure 1 shows the surface topography of a partially-grown graphene film displaying three distinct growth features as illustrated in the 3D insets. From the phase contrast image (right), one can identify the materials covering the surface: graphene films and so-called buffer layers

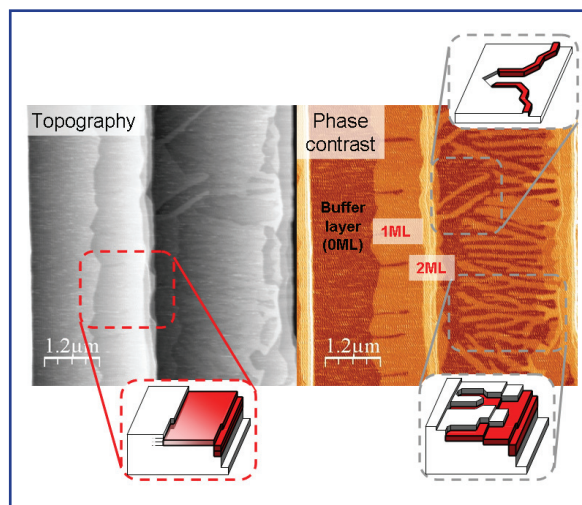


Figure 1: Morphology of SiC surfaces with growing graphene layers, acquired using atomic force microscopy (AFM). The left image is topography (grey scale), and the right image is the phase contrast (red-to-white scale). The steps go down from left to right. Phase contrast imaging is sensitive to the mechanical response of the material surface, and therefore is used as a fingerprint to distinguish a single graphene layer (1 ML), two layers (2 ML), and the interface layer formed during graphitization. Three distinct growth features are highlighted and schematically illustrated in the 3D insets, where the surfaces colored in red are terminated by graphene layers, and the ones in white are buffer layers (also indicated in the phase image). The surface composition is independently determined using LEEM, whose image contrast depends on the electronic structure of the material at the surface.

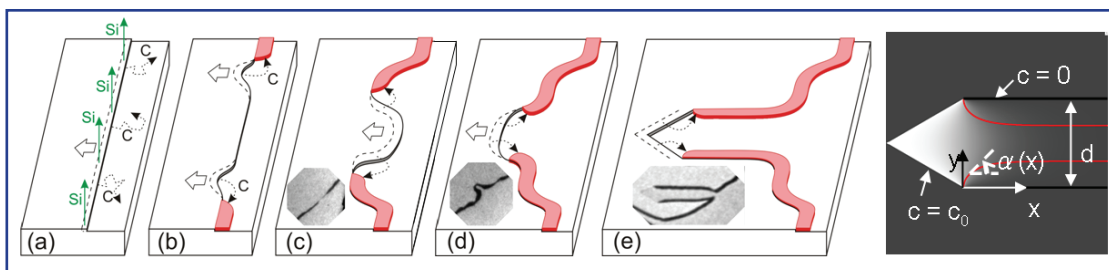


Figure 2: Schematics of the formation of an arrow feature and the calculated surface carbon atom concentration map. The process starts with sublimation of silicon atoms and formation of carbon atoms at the step edge (a). Once small patches of graphene are formed at the step edge, they grow in to ribbons of graphene decorating the step edges (b, c). When two ribbons meet, they turn and grow into the terrace given the limited number of carbon atoms emitted from the undecorated step edge (d, e). Some intermediate states have been detected in LEEM (insets in c-e) supporting this scenario. The LEEM images are (c) $2 \times 2 \mu\text{m}^2$, (d) $2 \times 2 \mu\text{m}^2$, and (e) $4 \times 2 \mu\text{m}^2$. The surface carbon atom concentration shown in the far right image is calculated by solving the time-dependent diffusion equation for the arrow geometry. The white area denotes higher carbon atom concentration. The red lines are the calculated boundaries of the resulting graphene ribbons, reproducing the experimentally-observed shape.

(precursor of a graphene film) separated by the atomic steps. The atomic steps originate from atomic-scale misalignment of a crystal plane and the polished substrate, commonly found on monolithic crystal surfaces. The left 3D inset (with a red boundary) features “step-flow growth” that turns three units of SiC into one layer (1 ML) of graphene. The right insets (with grey boundaries) are an “arrow feature” (up) and a “finger feature” (down) developed at the single atomic steps of SiC.

The analysis of “arrow features” provides much insight into how carbon diffuses on the surface during the synthesis process. Based on the surface topography surrounding arrow features, the sequence of its formation was deduced (details in Figure 2). The growth of arrow features (or the elongation of the shaft) can also be described analytically by solving the diffusion equation in an arrow geometry (far right in Figure 2). This reproduces the final geometry of an arrow feature, and shows the development of the concentration gradient of the surface carbon atoms inside an arrow shape during the growth. It also means that the diffusion of carbon atoms emitted at the atomic steps of buffer layer surfaces is the key factor in shaping the unique arrow geometry. Unfortunately, the diffusion-driven growth process leads to an unfavorable film morphology that cannot be controlled.

An entirely different mechanism is happening in “step-flow growth,” which converts three units of SiC to 1 ML of graphene. This mechanism was captured by a low-energy electron microscope (LEEM) in real-time at elevated temperature (details in Figure 3). The clear boundary between buffer layers and 1 ML of graphene, and the evolution of the boundaries, indicates that buffer layers are transformed to 1 ML graphene at the boundaries (as depicted schematically in the right illustration in Figure 3). Unlike the arrow feature, step-flow growth does not involve much carbon diffusion because carbon atoms emitted at the growth fronts are immediately turned into a graphene layer. Most importantly, step-flow growth creates homogeneous uninterrupted graphene films over a micrometer scale, which is promising for electronic device fabrication.

This work establishes a well-defined spatial relationship between the formation of carbon atom precursors and the growth of graphene. It is set by the starting configuration of the atomic steps of the buffer layer surface. Clearly, step-flow growth is the preferred mechanism to produce large-area graphene films. The next step is to clarify if, and how, different growth mechanisms alter the properties of this one-atom-thick material. Ultimately, the goal is to control the growth over an entire SiC substrate.

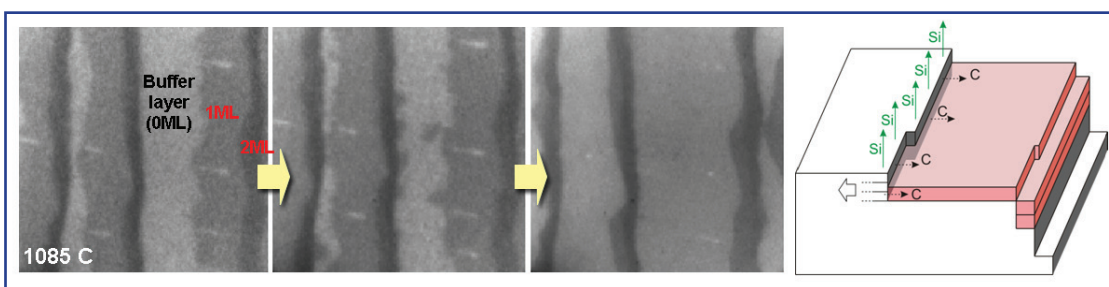


Figure 3: Step-flow growth of graphene. Left images ($3.5 \times 3.5 \mu\text{m}^2$) were obtained in real time with LEEM. The dark gray regions consist of 2 ML graphene, the medium gray regions are 1 ML, and the light gray regions are buffer layer. The right schematic illustrates the topography of step-flow growth. Triple bilayers of SiC (dotted lines) are transformed into 1 ML graphene.

Materials Science and Technology

Hydrogen Storage

Hydrogen Storage Research in the Metal Hydride Center of Excellence

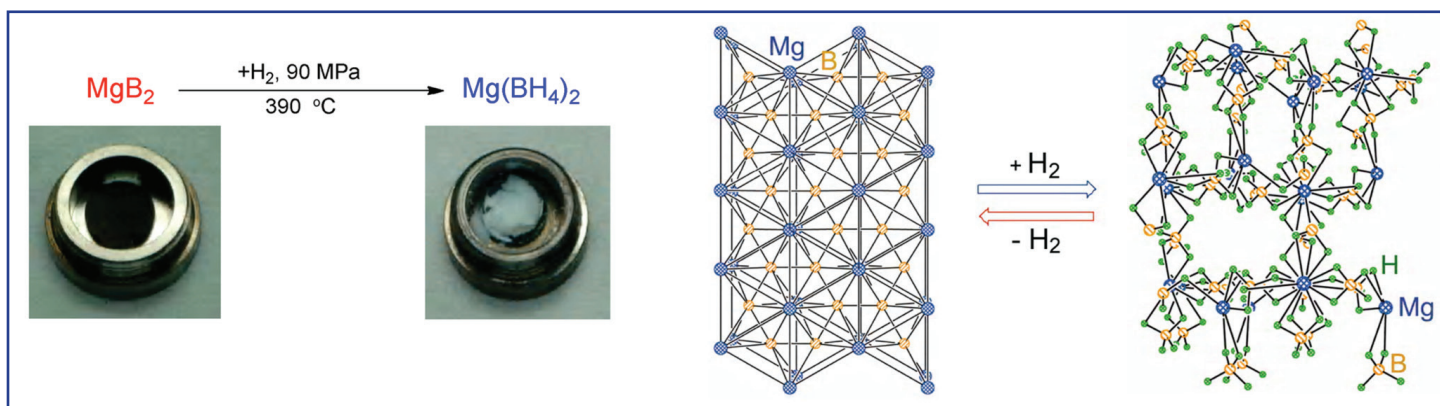


Figure 1: Storing hydrogen in magnesium borohydride.

Significant advances have been made with metal borohydride materials, but reversibility challenges still remain.

For more information:

Technical Contacts:

Vitale Stavila
925-294-3059
vnstavi@sandia.gov

Lennie Klebanoff
925-294-3471
lekleba@sandia.gov

Science Matters Contact:

Alan Burns
505-844-9642
aburns@sandia.gov

Hydrogen has the potential to be a major alternative to fossil fuels in the effort to reduce global warming. It can be reacted electrochemically with oxygen within a proton exchange membrane fuel cell to produce only water and clean power for electric motors with ~50% efficiency. In addition, hydrogen is abundant and has almost three times the gravimetric energy density of gasoline. Thus, a hydrogen-based economy has been discussed for many years. However, a critical obstacle in the widespread application of hydrogen fuel cell technology, especially for light-duty vehicles, is the lack of a convenient, safe, and efficient method to store hydrogen gas. While the most likely short-term solution to this problem is to store hydrogen as a flammable gas in composite pressure vessels, the development of new solid-state hydrogen storage systems would have a major impact on future automotive uses of hydrogen. Significant efforts are being directed toward finding one material with all the requisite properties for practical hydrogen storage. Many of those efforts have been coordinated by Sandia as the lead laboratory of the Metal Hydride Center of Excellence (MHCoE).

The MHCoE is a 17-institution organization (eight universities, six national laboratories, and three companies) funded out of the Department of Energy's Office of Energy Efficiency and Renewable Energy. The goal of the MHCoE is to find a storage material that can release (desorb) hydrogen when it is needed with very little energy input, and can rapidly adsorb hydrogen during re-fueling. One major area of hydrogen storage research at Sandia for the MHCoE is complex metal hydrides, including metal borohydrides, amides and alanates. Complex metal hydrides have always had exceptional volumetric and gravimetric densities, yet their high thermal stabilities have excluded them from consideration as practical, on-board hydrogen storage materials. Among complex hydrides, metal borohydrides exhibit the highest hydrogen storage capacities (up to 18.5 wt%, 121 kg/m³ for LiBH_4). In particular, magnesium borohydride, $\text{Mg}(\text{BH}_4)_2$ is one of the most promising borohydrides that stores an impressive 14.9 wt% hydrogen by weight (References 1,2). The material can be produced by hydrogenation of magnesium diboride pressed into pellets (Figure 1, left),

which involves transformation of hexagonal P_6/mmm MgB_2 into orthorhombic $Fddd$ $Mg(BH_4)_2$ (Figure 1, right).

Sandia has been studying several metal borohydride materials including lithium, magnesium and calcium borohydrides; however, full reversibility in these materials is problematic. A key to their successful use for hydrogen storage is the ability to tailor their composition, structure and morphology, as well as to control their size-dispersion and surface functionality. One such strategy is to improve the sorption/desorption reversibility properties with additives. As shown in Figure 2, addition of small amounts of scandium trichloride/titanium trifluoride to $Mg(BH_4)_2$ results in a dramatic improvement in the kinetics of hydrogen desorption with ~10 wt% H_2 released at 300 °C (Reference 1).

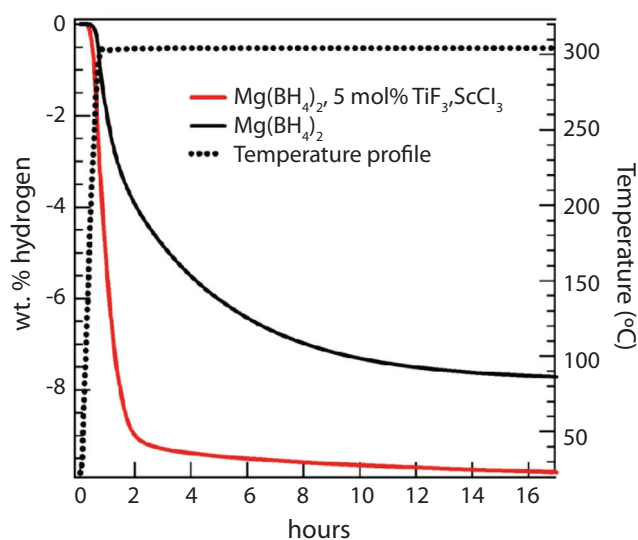


Figure 2: Temperature-programmed hydrogen desorption data for $Mg(BH_4)_2$ with 5 mol% TiF_3 and $ScCl_3$ (red curve) and pure $Mg(BH_4)_2$ (black curve) heated to 300 °C.

The decomposition of metal borohydrides during desorption is a complex process. One important limitation in using borohydride materials is the formation of stable intermediates such as dodecahydro-closo-dodecaborates ($MgB_{12}H_{12}$). Sandia has developed two strategies to mitigate this problem. One solution is to destabilize the intermediates thermodynamically, for instance CaH_2 decreases the decomposition temperature of $CaB_{12}H_{12}$ by more than 200 °C (Reference 3). Another strategy is to hydrogenate the intermediates, forming starting metal borohydrides. Almost full conversion of $Li_2B_{12}H_{12}$ into $LiBH_4$ can be achieved at high hydrogen pressures in the presence of stoichiometric amounts of lithium hydride (Figure 3).

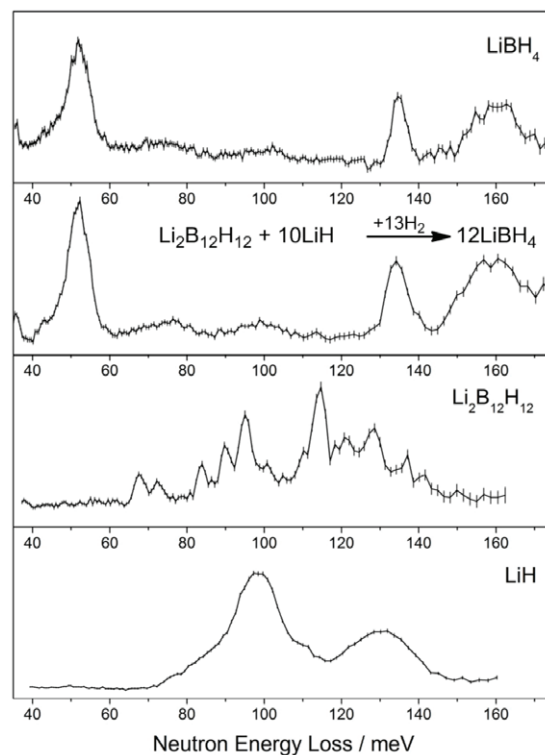


Figure 3: Neutron vibrational spectroscopy data showing full conversion of ball-milled $Li_2B_{12}H_{12} + 10LiH$ composite into $LiBH_4$.

Significant advances have been made at the MHCoe to improve the hydrogen storage characteristics of metal borohydrides. Several materials from this class of compounds have higher volumetric densities than gaseous or liquid hydrogen. The key to enable effective hydrogen storage in these materials is to improve the reversibility using destabilization, catalysis and nanoengineering approaches.

References

1. R.J. Newhouse, V. Stavila, S.J. Hwang, L.E. Klebanoff, J.Z. Zhang, Reversibility and improved hydrogen release of magnesium borohydride, *J. Phys. Chem. C*, (2010) **114**, 5224–5232.
2. G. Severa, E. Ronnebro, C.M. Jensen, Direct hydrogenation of magnesium boride to magnesium borohydride: demonstration of > 11 weight percent reversible hydrogen storage, *Chem. Commun.*, (2010) **46**, 421–423.
3. V. Stavila, J.H. Her, W. Zhou, S.J. Hwang, C. Kim, L.A.M. Ottley, T.J. Udovic, Probing the structure, stability and hydrogen storage properties of calcium dodecahydro-closo-dodecaborate, *J. Solid State Chem.*, (2010) **183**, 1133–1140.



